

NO-A191 110

MICROWAVE SEMICONDUCTOR RESEARCH-MATERIALS DEVICES AND  
CIRCUITS(U) CORNELL UNIV ITHACA NY SCHOOL OF ELECTRICAL  
ENGINEERING L F EASTMAN ET AL. OCT 87 AFOSR-TR-87-2019

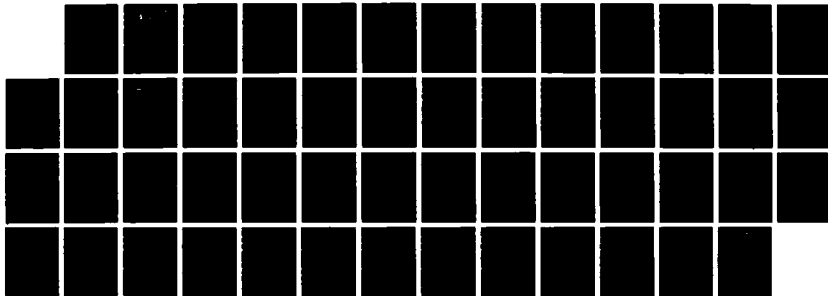
1/1

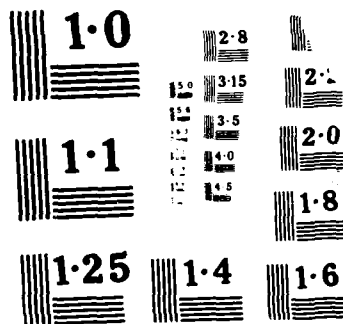
UNCLASSIFIED

F49620-84-C-0060

F/G 20/12

NL





Unclassified

(2)

AD-A191 118

## REPORT DOCUMENTATION PAGE

DTIC FILE COPY

Unclassified		DTIC		1B. RESTRICTIVE MARKINGS	
2A. SECURITY CLASSIFICATION AUTHORITY Unclassified		ELECTED		3. DISTRIBUTION/AVAILABILITY OF REPORT Unclassified/Unlimited	
2B. DECLASSIFICATION/DOWNGRADING SCHEDULE NA		1988			
4. PERFORMING ORGANIZATION REPORT NUMBER(S) AD				5. MONITORING ORGANIZATION REPORT NUMBER(S) AFOSR-TR- 87-2019	
6A. NAME OF PERFORMING ORGANIZATION Cornell University School of Elec. Engin.		6B. OFFICE SYMBOL (If applicable) 17E		7A. NAME OF MONITORING ORGANIZATION AFOSR	
6C. ADDRESS (City, State and ZIP Code) Ithaca, NY 14853				7B. ADDRESS (City, State and ZIP Code) BKI 410 BAFB DC 20332	
8A. NAME OF FUNDING/SPONSORING ORGANIZATION AFOSR		8B. OFFICE SYMBOL (If applicable)		9. PROCUREMENT INSTRUMENT IDENTIFICATION NUMBER F49620-84-C-0060	
8C. ADDRESS (City, State and ZIP Code) Building 410 Bolling Air Force Base Washington, DC 20332				10. SOURCE OF FUNDING NOS.	
		PROGRAM ELEMENT NO.		PROJECT NO.	TASK NO.
		61102F		2305	A9
11. TITLE (Include Security Classification) MICROWAVE SEMICONDUCTOR RESEARCH-MATERIALS, DEVICES AND CIRCUITS					
12. PERSONAL AUTHOR(S) L.F. Eastman, J.R. Shealy, D.W. Woodard, S. Mukherjee, G.W. Wicks, J.M. Ballantyne, C.I. Tang, G.J. Wolga, W.H. Ku, H.J. Carlin and J.D. Krusius					
13A. TYPE OF REPORT 3 year Final		13B. TIME COVERED FROM 5/1/84 TO 4/30/87		14. DATE OF REPORT (Yr., Mo., Day) October 1987	
				15. PAGE COUNT 50	
16. SUPPLEMENTARY NOTATION					
17. COSATI CODES		18. SUBJECT TERMS (Continue on reverse if necessary and identify by block number)			
FIELD	GROUP	SUB. GR.			
19. ABSTRACT (Continue on reverse if necessary and identify by block number)					
<p>This program covers the growth and assessment of gallium arsenide and related compounds and alloys for use in microwave, millimeter wave, and optical devices. It also covers the processing of the material into devices, the testing of the devices, and the theoretical modeling of carrier transport in these devices. Both molecular beam epitaxy (MBE) and organometallic vapor phase epitaxy (OMVPE) are used for growth. The following specific tasks are pursued:</p> <p>TASK 1 Develop an improved understanding of the role of the substrate and the growth parameters on the quality of device structures on GaAs and related materials grown by OMVPE.</p> <p>TASK 2 Investigate the frequency and power limits of power FET devices employing a two-dimensional electron gas in the channel.</p>					
20. DISTRIBUTION/AVAILABILITY OF ABSTRACT UNCLASSIFIED/UNLIMITED <input checked="" type="checkbox"/> SAME AS RPT. <input type="checkbox"/> DTIC USERS <input type="checkbox"/>		21. ABSTRACT SECURITY CLASSIFICATION Unclassified			
22A. NAME OF RESPONSIBLE INDIVIDUAL L.F. Eastman/J.P. Krusius		22B. TELEPHONE NUMBER (Include Area Code) (607) 255-4369/3401		22C. OFFICE SYMBOL 17E	

Approved For \_\_\_\_\_  
 NAME GRA&I \_\_\_\_\_ ✓  
 TITLE TABS \_\_\_\_\_ ☐  
 Date Submitted \_\_\_\_\_ ☐  
 Initials \_\_\_\_\_

---

By \_\_\_\_\_  
 Title \_\_\_\_\_

---

Date \_\_\_\_\_  
 By \_\_\_\_\_  
 Title \_\_\_\_\_

A-7

DTIC  
COPY  
ASPECTED

0100 000 000 000 000

- 2

**AFOSR-TR- 87 - 2019**

**THREE YEAR FINAL REPORT**

***MICROWAVE SEMICONDUCTOR RESEARCH -  
MATERIALS, DEVICES AND CIRCUITS***

**MAY 1, 1984 - APRIL 30, 1987**

**CONTRACT # F49620-84-C-0060**

## **TABLE OF CONTENTS**

	<b><u>PAGE</u></b>
TASK 1 <i>THE OMVPE GROWTH AND CHARACTERIZATION OF GaAs AND RELATED MATERIALS FOR HIGH PERFORMANCE ELECTRON DEVICES</i> L.F. Eastman and J.R. Shealy	4
TASK 2 <i>FUNDAMENTAL STUDY OF THE PERFORMANCE LIMITS OF HIGH FREQUENCY GaAs FET's</i> L.F. Eastman, D.W. Woodard and S.D. Mukherjee	10
TASK 3 <i>MBE GROWN-LATTICE-MATCHED HETEROJUNCTION FOR IMPROVED TRANSISTORS</i> L.F. Eastman and G.W. Wicks	14
TASK 4 <i>HIGH SPEED AMPLITUDE MODULATION OF SEMICONDUCTOR LASERS AND LIGHT EMITTING DIODES</i> L.F. Eastman and G.W. Wicks	17
TASK 5 <i>HIGH SPEED RECEIVERS FOR OPTICAL COMMUNICATIONS</i> J.M. Ballantyne	20
TASK 6 <i>SPECTRAL AND DYNAMIC CHARACTERISTICS OF SEMICONDUCTOR MATERIALS AND STRUCTURES</i> C.L. Tang	27
TASK 7 <i>CARRIER DYNAMICS IN COMPOUND SEMICONDUCTORS STUDIED WITH PICOSECOND OPTICAL EXCITATION</i> G.J. Wolga	32
TASK 8 <i>ADVANCED DESIGN TECHNIQUES FOR MICROWAVE GaAs FET AMPLIFIERS</i> W.H. Ku	37
TASK 9 <i>WIDEBAND CIRCUITS AND SYSTEMS</i> H.J. Carlin	44
TASK 10 <i>DEVICE SIMULATION AND CIRCUIT MODELING FOR III-V DEVICES IN THE BOUNDARY LIMITED HIGH FIELD TRANSPORT REGIME</i> J.P. Krusius	45

## **TASK 1 THE OMVPE GROWTH AND CHARACTERIZATION OF GaAs AND RELATED MATERIALS FOR HIGH PERFORMANCE ELECTRON DEVICES**

L.F. Eastman and J.R. Shealy

### **OBJECTIVE**

The overall program objective is to develop an improved understanding of the role of the substrate and the growth parameters on the quality of device structures on GaAs and related materials grown by Organometallic Vapor Phase Epitaxy (OMVPE).

### **DISCUSSION OF STATE-OF-THE-ART**

The OMVPE technique has evolved into a technology capable of producing high purity epitaxial films and related structures with interfaces which are atomically abrupt in many cases. There is evidence from Raman spectroscopy of GaAs/AlAs superlattice structures that at the same growth rate and substrate temperature the OMVPE technique actually produces sharper interfaces than the older MBE technology. The problem remains to be carbon contamination from the organometallic source which limits the purity of films, especially those containing aluminum. Since the OMVPE technique readily address the growth of phosphides, antimonides, and other new III-V alloys and structures, there remains to be a large volume of research which has yet to be addressed.

### **PROGRESS**

The OMVPE research effort at Cornell has centered around the growth and characterization of GaAs, AlGaAs, GaInP and their heterostructures. Experiments related to heterojunction interface abruptness have shown interface widths  $< 10 \text{ \AA}$  in GaAs/AlGaAs quantum wells. In modulation doped structures, a 2DEG mobility of  $7000 \text{ cm}^2/\text{v-sec}$  at 300 K (sheet density  $1.0 \times 10^{12} \text{ cm}^{-2}$ ) and  $70,000 \text{ cm}^2/\text{v-sec}$  at 77 K (sheet density  $8.0 \times 10^{11} \text{ cm}^{-2}$ ) have been recorded. These structures were grown at  $625^\circ\text{C}$  using trimethyl metals, with V/III = 20 for GaAs and 250 for AlGaAs (to reduce carbon incorporation). Spacer thickness is  $150 \text{ \AA}$ , and Te was used as the n-type dopant. Temperature variable Hall measurements show a leveling off of mobility and sheet concentration below 50 K, indicative of good 2DEG confinement and showing that performance is limited by AlGaAs purity.

Progress has been made on the growth by Organometallic Vapor Phase Epitaxy (OMVPE) and characterization of GaInP, AlInP and GaInP/GaAs heterostructures. GaInP will be useful in the following devices: as an active layer material in a visible laser, as an emitter in a GaInP/GaAs bipolar transistor, and as a doped region in the GaInP/GaAs MODFET. Its useful properties include a large, direct bandgap (1.9 eV, lattice match), higher purity than OMVPE AlGaAs is possible, and absence of carbon or problems associated with AlGaAs. In our early lattice match and calibration growths of GaInP, we observed a lattice matched bandgap of 1.83 eV (lattice match determined by photoluminescence linewidths and morphology). This is far lower than the expected value of 1.91 eV which has been reported in the literature. This was blamed on compositional fluctuations during growth due to the trimethylgallium flow controller being operated in the noisy region below 5% full scale. The flow controller has since been replaced with one of a more suitable full scale flow and the compositional fluctuation problems have been alleviated.



The narrowest observed 300 K PL half-width is 49 meV (18 meV at 4 K). This is rather broad, and could be attributed to low purity. Our trimethylindium (TMIn) source is known to be contaminated, giving a background doping for InP and GaInP epilayers of low  $10^{16}\text{cm}^{-3}$ . Mobilities of the GaInP are about  $2000\text{ cm}^2/\text{v}\cdot\text{sec}$  at 300 K and about  $5000\text{ cm}^2/\text{v}\cdot\text{sec}$  at 77 K, comparable to values reported by other workers. Replacing the TMIn source with one of higher purity should produce higher purity epitaxial material with narrower PL peaks. This is one of our plans for future work, especially for microwave device work where high purity is necessary.

GaInP epilayers have been characterized by photoluminescence, Nomarski phase contrast microscopy, Raman scattering spectroscopy, Hall measurements, and capacitance-voltage measurements. Photoluminescence and morphology studies have been most useful in determining lattice match. If thick (1 micron) epilayers are slightly gallium rich (lattice mismatch  $\Delta a/a < -0.001$ ), the epilayer is under tensile strain. As a result, cracks along (110) are formed to relieve the strain. The formation of these cracks is very sensitive to mismatch on the tension (Ga-rich) side, and the appearance of these cracks is a clear indication of lattice mismatch with the epilayer under tension.

Raman studies of GaInP epilayers have also been useful and interesting. In the Raman spectrum, the GaP-like LO phonon peak, as well as the InP-like LO phonon peak has been observed and its energy measured as a function of composition. A TO peak has also been measured, but has not been associated with an InP-like mode or a GaP-like mode. Raman shifts have also been measured as a function of temperature, measuring the decomposition temperature of GaInP. The Raman signal disappears as the surface decomposes from the excess desorption of phosphor. The temperature at which this occurs in  $\text{Ga}_{0.5}\text{In}_{0.5}\text{P}$  is about  $500^\circ\text{C}$ .

AlInP will be useful as a cladding layer for the visible laser. Also, we hope to simulate the intermediate lattice matched alloy  $(\text{Al}_x\text{Ga}_{1-x})_{0.5}\text{In}_{0.5}\text{P}$  with a short-period-superlattice of  $\text{Al}_{0.5}\text{In}_{0.5}\text{P}/\text{Ga}_{0.5}\text{In}_{0.5}\text{P}$ ; this to be used as a separate confinement region in a quantum well laser, with the advantage of simpler lattice matching of ternary compounds compared to the uniform quaternary alloy. Knowledge of AlInP will also be helpful in growing the quaternary alloy for use in microwave devices. Trading off aluminum for gallium in GaInP will increase the band discontinuity at a heterojunction with GaAs, thus making the alloy  $(\text{Al}_x\text{Ga}_{1-x})_{0.5}\text{In}_{0.5}\text{P}$  an improvement over  $\text{Ga}_{0.5}\text{In}_{0.5}\text{P}$  when used in the transistor devices mentioned earlier.

Formation of the GaInP/GaAs heterostructure will be important in the MODFET and HBT structures. To study the interface, a series of  $\text{Ga}_{0.5}\text{In}_{0.5}\text{P}$  (75 Å/GaAs (75 Å) superlattices were grown. In one set of samples, different growth stop procedures were used at the interfaces: 1) continuous growth, 2) 9 second growth stop under group V gas, and 3) 9 second growth stop under group V gas followed by 5 second purge of all reactants. Transmission electron micrographs of each sample show good contrast between the layers, and compositional uniformity within the layers. However, TEM cannot give accurate information about the superlattice compositional profile, as can Raman spectroscopy and photoluminescence. Both Raman and PL studies show very little difference between superlattices grown continuously and those grown with a 9 second growth stop under group V gas at the interfaces. This means either 1) any alloying taking place involves only the group V element (for example, As in the GaInP or P in the GaAs), or 2) a 9 second growth stop is insufficient in completely stopping growth, thus

leading to a group III element carry over. Possibility (1) would give an increase in the superlattice energy gap, while possibility (2) would lead to a decrease in the superlattice energy gap. We have observed a lower PL energy than expected, so we believe that longer growth stops are required to completely stop growth.

The superlattice grown with a growth stop and purge at the interfaces showed a PL energy close to the expected value (calculated using a Kronig-Penney model with assumptions made concerning effective masses within each material), so it seems that the growth stop together with complete purge is successful in stopping the group III carry over. However, the Raman spectrum contained forbidden TO peaks, and also the PL linewidth was larger than that of the other two samples. This suggests a poor interface, possibly due to decomposition of GaInP during the purge, since the growth temperature (625°C) is well above the decomposition temperature of GaInP.

A other series of three lattice mismatched superlattices were also studied to investigate the distribution of strain. One superlattice was unstrained (lattice matched), and one each with GaInP under compression and strain. For each sample, the GaAs LO peak was shifted by about 4 cm<sup>-1</sup>, due to compositional intermixing. The shift of GaP-like LO phonon depended on the state of strain in the sample. These measurements show that most of the strain occurs in the GaInP with little strain in the GaAs.

To determine the effective interfacial thickness over which alloying occurs, a set of GaAs/Ga<sub>0.5</sub>In<sub>0.5</sub>P quantum wells was grown. In one sample, 4 wells were grown, with 2000 Å of GaInP barrier between them. The well thicknesses were 150 Å, 75 Å, 40 Å and 15 Å, with the thicker wells near the substrate, and all interfaces grown with a 5 second growth stop under group V gas. PL was observed from the 150 Å and 75 Å wells, with each peak shifted significantly due to alloy intermixing, and the 75 Å well peak being very broad. No PL was observed from the 40 Å or 15 Å well, thus leading to a conclusion that the interfacial alloying thickness is approximately 40 Å.

Several GaInP/GaAs MODFET structures were grown. In a first attempt, a MODFET with 150 Å undoped spacer was grown. Hall mobilities at 300 K and 77 K indicated conduction in the doped GaInP ( $\mu = 1000$  cm<sup>2</sup>/v-sec at 300 K and  $\mu = 2500$  cm<sup>2</sup>/v-sec at 77 K). To increase charge transfer into the interfacial 2-D electron gas (2DEG), two techniques were tried: 1) decreasing the spacer thickness to 50 Å and 0 Å, and 2) growing the GaInP slightly Ga-rich (deliberately off lattice match), thus increasing the conduction band discontinuity to aid charge transfer. Neither of these methods improved the result, and we now believe this is due to excessive interfacial alloying. In the future we would like to take steps to reduce this alloying, namely 1) growth of GaAs buffer at lower growth rate, and 2) a longer growth stop at the interface. If this is successful in giving good 2DEG confinement, then this, along with using a higher purity TMIn source should give a better MODFET result than the AlGaAs/GaAs MODFET by OMVPE (due to higher purity GaInP as compared to OMVPE AlGaAs) with the added benefit of there being no deep donor problems associated with lattice matched GaInP.

Growth of Al<sub>x</sub>In<sub>1-x</sub>P has also been studied. Lattice matching to GaAs substrates is achieved using a surface morphology study of a series of 1 micron layers near lattice match. A high growth temperature (700-720°C) and high V/III ratio produces lattice matched epilayers with featureless surfaces. The optical properties of Al<sub>x</sub>In<sub>1-x</sub>P were studied using electroreflectance and Raman

spectroscopy. Using electroreflectance to measure the direct ( $E_0$ ) bandgap of the epitaxial layers, the compositional dependence of the direct bandgap energy was determined. A concave upward bowing was found, in contrast to the exactly linear dependence measured in early work on  $\text{Al}_x\text{In}_{1-x}\text{P}$ , but similar to the bowing in most other compound semiconductor ternaries. In the Raman scattering spectrum, a two-mode behavior is observed, similar to that observed in  $\text{Al}_x\text{Ga}_{1-x}\text{As}$  and  $\text{Ga}_x\text{In}_{1-x}\text{P}$ . The composition dependence of the AlP-like LO mode in  $\text{Al}_x\text{In}_{1-x}\text{P}$  extrapolates to the LO phonon frequency of bulk AlP. Resonant Raman scattering is also performed on the  $\text{Al}_x\text{In}_{1-x}\text{P}$  epilayers. Raman measurements performed with the various lines from an argon laser demonstrate that the Raman signal intensity is greatly increased when the laser excitation energy closely matches the direct bandgap of the material under examination. In this case, the laser line energy which results in the greatest Raman intensity agrees very well ( $\pm 20$  meV) with the direct bandgap energy measured by electroreflectance.

Dopant behavior in  $\text{Al}_{0.5}\text{In}_{0.5}\text{P}$  has been investigated. It was determined that tellurium n-type dopant is activated at room temperature, but significant freeze-out of the donors occurs at 77 K, indicative of a donor binding energy of about 60 meV. p-type doping using zinc was attempted, but no activation was observed at room temperature. By alloying the  $\text{Al}_{0.5}\text{In}_{0.5}\text{P}$  with  $\text{Ga}_{0.5}\text{In}_{0.5}\text{P}$ , however, the zinc became an active acceptor at 300 K due to the decreased acceptor binding energy in the alloy compared to  $\text{Al}_{0.5}\text{In}_{0.5}\text{P}$ .

Strained  $\text{Ga}_x\text{In}_{1-x}\text{P}/\text{Al}_y\text{Ga}_{1-y}\text{P}$  quantum wells were grown in an attempt to study high energy luminescence structures. First, growth of  $\text{Al}_x\text{Ga}_{1-x}\text{P}$  was optimized. Growth of this material required very high growth temperatures (greater than  $825^\circ\text{C}$ ) for smooth surfaces. Strained  $\text{Ga}_x\text{In}_{1-x}\text{P}$  ( $0.4 < x < 0.5$ )/GaP quantum well structures grown at  $750^\circ\text{C}$ , however, produced no detectable emission, even at 4 K. Sputter Auger electron spectroscopy composition profiles of these structures revealed that the GaInP quantum wells had completely interdiffused with the GaP cladding layers, resulting in a uniform GaInP alloy. To alleviate this problem, growth of the strained quantum well structure was performed at  $700^\circ\text{C}$ , which tends to produce GaP layers with rough surfaces. The intermixing problem still appeared, however, even at this growth temperature. It is believed that lowering the growth temperature further could produce well defined quantum wells, but would also lead to very rough GaP surfaces. A possible solution is atomic layer epitaxy, which reportedly permits growth of smooth epilayers at drastically reduced growth temperatures.

#### **SCIENTIFIC IMPACT OF RESEARCH**

With many III-V compounds and structures yet to be explored, this materials and related device effort provides an experimental basis for the evaluation and understanding of electron transport and confinement of new high velocity semiconductor materials and structures. In characterizing new materials, the structural properties will be detailed such that the feasibility for the growth of many proposed structures will be determined.

#### **DEGREES**

Ph.D., C.F. Schaus, January 1986

"Optoelectronic Devices and Materials Grown by Organometallic Vapor Phase Epitaxy"

## PUBLICATIONS

1. "Graded Band-Gap AlGaAs Solar Cells Grown by Organometallic Vapor Phase Epitaxy", D.K. Wagner and J.R. Shealy, Proc. Photovoltaics Specialists Conf., Orlando, FL (May 1-4, 1984).
2. "Graded Band-Gap p/n AlGaAs Solar Cells Grown by Organometallic Vapor Phase Epitaxy", D.K. Wagner and J.R. Shealy, Appl. Phys. Lett., **45** (2) 162-164 (July 1984).
3. "High External Efficiency (36%) 5-Micron Mesa Isolated GaAs Quantum Well Laser by Organometallic Vapor Phase Epitaxy", D.F. Welch, C.F. Schaus and J.R. Shealy, Appl. Phys. Lett., **46** (2) 121-123 (Jan. 1985).
4. "Investigation of the Properties of OMVPE Grown AlGaAs/GaAs Heterostructures Using Raman Scattering", J.R. Shealy, C.F. Schaus and G.W. Wicks, Appl. Phys. Lett., **47** (2) 125-127 (July 1985).
5. "TEM Observations of Compositional Variations in  $\text{Al}_x\text{Ga}_{1-x}\text{As}$  Grown by OMVPE", K-H. Kuesters, B.C. DeCooman, J.R. Shealy and C.B. Carter, J. Crystal Growth, **71**, 514-518 (1985).
6. "OMVPE Growth of GaAs/(AlGa)As Integrated Optical Devices", C.F. Schaus, J.R. Shealy, F.E. Najjar and L.F. Eastman, 12th Int. Symp. on GaAs and Related Cpd., Karuizawa, Japan (Sept. 23-26, 1985).
7. "Improved GaAs/AlGaAs Quantum Well Heterostructures by Organometallic Vapor Phase Epitaxy", C.F. Schaus, J.R. Shealy, L.F. Eastman, B.C. DeCooman and C.B. Carter, J. Appl. Phys., **59** (2) 678-680 (Jan. 1986).
8. "Organometallic Vapor Phase Epitaxial Growth of GaInP/GaAs (AlGaAs) Heterostructures", J.R. Shealy, C.F. Schaus and L.F. Eastman, Appl. Phys. Lett., **48** (3) 242-244 (Jan. 1986).
9. "Integrated Laser/Phototransistor Optoelectronic Switching Device by Organometallic Vapor Phase Epitaxy", C.F. Schaus, J.R. Shealy, F.E. Najjar and L.F. Eastman, Elec. Lett., **22** (9) 454-456 (April 1986).
10. "Characterization by Raman Spectroscopy of GaInP, AlInP and GaAs Single Layers and Superlattices", presented at Int. Symp. GaAs and Related Cpd., Las Vegas, NV (1986); Inst. Phys. Conf. Series, **83** (4) 257 (1987).
11. "Graded-Index Separate-Confinement InGaAs/GaAs Strained-Layer Quantum Well Laser Grown by Metalorganic Chemical Vapor Deposition", D. Fekete, K.T. Chan, J.M. Ballantyne and L.F. Eastman, Appl. Phys. Lett., **49** (24) 1659-1660 (Dec. 1986).
12. "GaAs/GaAlAs Quantum Well Laser with a Lateral Spatial Variation in Thickness Grown by Metalorganic Chemical Vapor Deposition", D. Fekete, D. Bour, J.M. Ballantyne and L.F. Eastman, Appl. Phys. Lett., **50** (11) 635-637 (March 1987).

13. "Ridge Waveguide Injection Laser with a GaInAs Strained-Layer Quantum Well ( $\lambda = 1 \mu\text{m}$ )", S.E. Fischer, D. Fekete, G.B. Feak and J.M. Ballantyne, Appl. Phys. Lett., **50** (12) 714-716 (March 1987).
14. "Optical Properties of  $\text{Al}_x\text{In}_{1-x}\text{P}$  Grown by Organometallic Vapor Phase Epitaxy", D.P. Bour, J.R. Shealy, G.W. Wicks and W.J. Schaff, Appl. Phys. Lett., **50** (10) 615-617 (March 1987).
15. "Investigation by Raman Scattering of the Properties of III-V Compound Semiconductors at High Temperature", J.R. Shealy and G.W. Wicks, Appl. Phys. Lett., **50** (17) 1173-1175 (April 1987).
16. "Ga<sub>0.5</sub>In<sub>0.5</sub>P/GaAs Interfaces by OMVPE", D.P. Bour, J.R. Shealy and S. McKernan, submitted to Appl. Phys. Lett. (June 1987).
17. "High Power (1.4 watt) AlGaInP Graded Index Separate Confinement Heterostructure Visible ( $\lambda \sim 658 \text{ nm}$ ) Laser", D.P. Bour and J.R. Shealy, submitted to Appl. Phys. Lett. (July 1987).

## **TASK 2    *FUNDAMENTAL STUDY OF THE PERFORMANCE LIMITS OF HIGH FREQUENCY GaAs FET's***

L.F. Eastman, D.W. Woodard and S.D. Mukherjee

### **OBJECTIVE**

Determine the fundamental physical electronics limits on performance of short gate high frequency modulation doped AlGaAs/GaAs power FET's with 0.5 micron and shorter gates.

### **DISCUSSION OF STATE-OF-THE-ART**

In conventional MODFET structures both the 2-D electron-gas density and the breakdown voltage are limited. If doping in the AlGaAs is increased to raise the sheet density, parallel conduction in the AlGaAs and reduced depletion depth and consequently reduced breakdown voltage become limiting factors. To understand these effects, quantitatively modeling of charge control and modulation efficiency in MODFETs has been done and double heterostructures with pulsed doping have been made to extend the limits.

### **PROGRESS**

In order to model MODFET structures, a figure of merit, the modulation efficiency, was introduced. The modulation efficiency gives an indication of the charge control limited  $f_T$  as a function of 2DEG density. The effect of epilayer design parameters on the modulation efficiency was studied via a classical charge control model which incorporates Fermi-Dirac statistics and Al composition dependent donor energies, and gives excellent agreement with quantum mechanical calculations. The modulation efficiency, ME, is related to  $f_T$  by the following:

$$f_T = ME V_{eff} / 2\pi L_g$$

where  $V_{eff}$  is the effective velocity of the 2DEG. Figure 1 shows the modulation efficiency as a function of 2DEG sheet density for various aluminum fractions. The decrease in  $f_T$  predicted by this model is in qualitative agreement with experimental data. Note that there is no increase in ME above 30% Al while lower Al fractions degrade the ME. Figure 2 shows the effect of spacer layer thickness which is to decrease the ME.

To circumvent the problems of conventional MODFET designs, planar-doped double heterojunction MODFET's were fabricated with 0.5 micron by 200 micron gate geometry. An  $f_T$  of 24 GHz with corresponding  $f_{max}$  of 50 GHz was achieved. The room temperature DC characteristics show a very broad  $g_m$  peak of 135 mS/mm with a maximum channel current of 350 mA/mm. Power measurements on these devices showed a maximum efficiency of 47% with 5.5 dB associated gain and 0.5 W/mm. At 77 K there was very little light sensitivity and no I-V collapse.

### **SCIENTIFIC IMPACT OF RESEARCH**

The impact of this work has been improved understanding of factors limiting the performance of conventional MODFET structures and achievement of device

performance exceeding these limitations through use of double heterojunction structures.

### DEGREES

1. C.M. Lowe, Ph.D., August 1984  
"A Study of Breakdown Voltage for Gallium Arsenide Power Transistors with Gate lengths in the Submicron Range"
2. J.C. Huang, Ph.D., January 1987  
"The Effect of MBE Growth Conditions and Heterostructure Designs on AlGaAs/GaAs MODFET Device Performance"

### JSEP PUBLICATIONS

1. "Very Low Resistance Ohmic Contact Fabrication for  $\text{Al}_{0.25}\text{Ga}_{0.75}\text{As}/\text{GaAs}$  and  $\text{Al}_{0.48}\text{In}_{0.52}\text{As}/\text{Ga}_{0.47}\text{In}_{0.53}\text{As}$  Lateral Devices: A Comparison", P. Zwicknagl, S.D. Mukherjee, W.L. Jones, H. Lee, P.M. Capani, T. Griem, J.D. Berry, L. Rathbun and L.F. Eastman, Inst. Phys. Conf. Ser. No. 74, Chapter 7, 581-586 (1985).
2. "Etching and Surface Preparation of GaAs for Device Fabrication", S.D. Mukherjee and D.W. Woodard, Chapter 4 in Gallium Arsenide, edited by M.J. Howes and D.V. Morgan, John Wiley & Sons, Ltd., 119-160 (1985).
3. "As<sub>2</sub> Ambient Activation and Alloyed Ohmic Contact Studies of Si<sup>+</sup> Ion Implanted  $\text{Al}_{0.3}\text{Ga}_{0.7}\text{As}/\text{GaAs}$  Modulation Doped Structures", S.D. Mukherjee, P. Zwicknagl, H. Lee, L. Rathbun and L.F. Eastman, Solid State Elec., **29** (2) 181-187 (Feb. 1986).
4. "Very Low Resistance Au/Ge/Ni/Ag Based Ohmic Contact Formation to  $\text{Al}_{0.25}\text{Ga}_{0.75}/\text{GaAs}$  and  $\text{Al}_{0.48}\text{In}_{0.52}\text{As}/\text{Ga}_{0.47}\text{In}_{0.53}\text{As}$  Heterostructures: A Behavioral Comparison", P. Zwicknagl, S.D. Mukherjee, P.M. Capani, H. Lee, H.T. Griem, L. Rathbun, J.D. Berry, W.L. Jones and L.F. Eastman, J. Vac. Sci. Tech., **B4** (2) 476-484 (March/April 1986).
5. "The Effect of Subband Quantization in the 2-D Electron Gas on Thermionic Current and Heterojunction Capacitance in an n- $\text{Al}_x\text{Ga}_{1-x}\text{As}/\text{n-GaAs}$  Heterojunction", Z. Greenwald, D.W. Woodard, P.J. Tasker and L.F. Eastman, Solid State Elec., **29** (11) 1099-1106 (Nov. 1986).

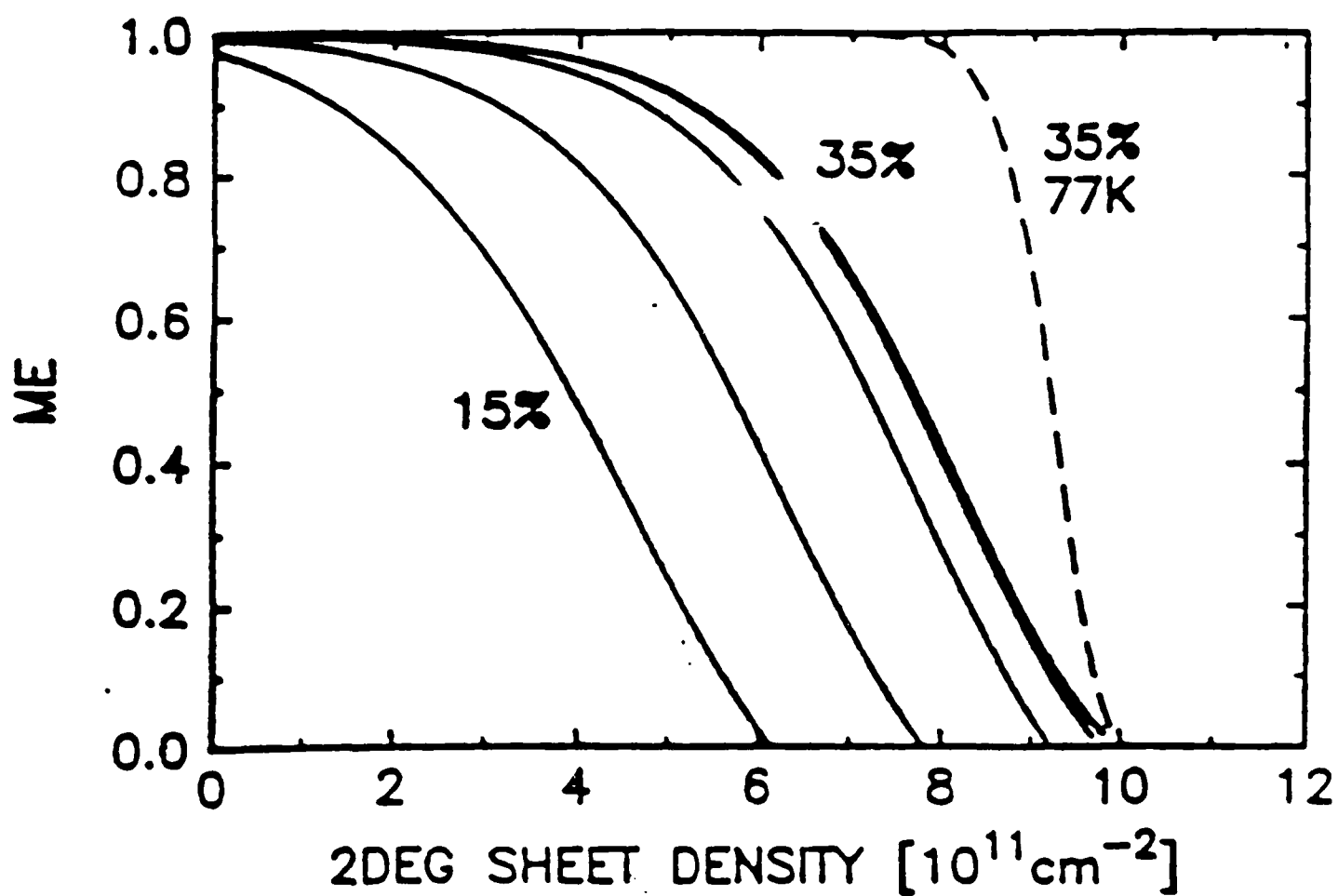


Figure 1. 300 K ME vs. 2DEG sheet density for 15, 20, 25, 30, and 35% AL (solid lines). For comparison, 77 K ME is also plotted for 35% Al (dashed line)



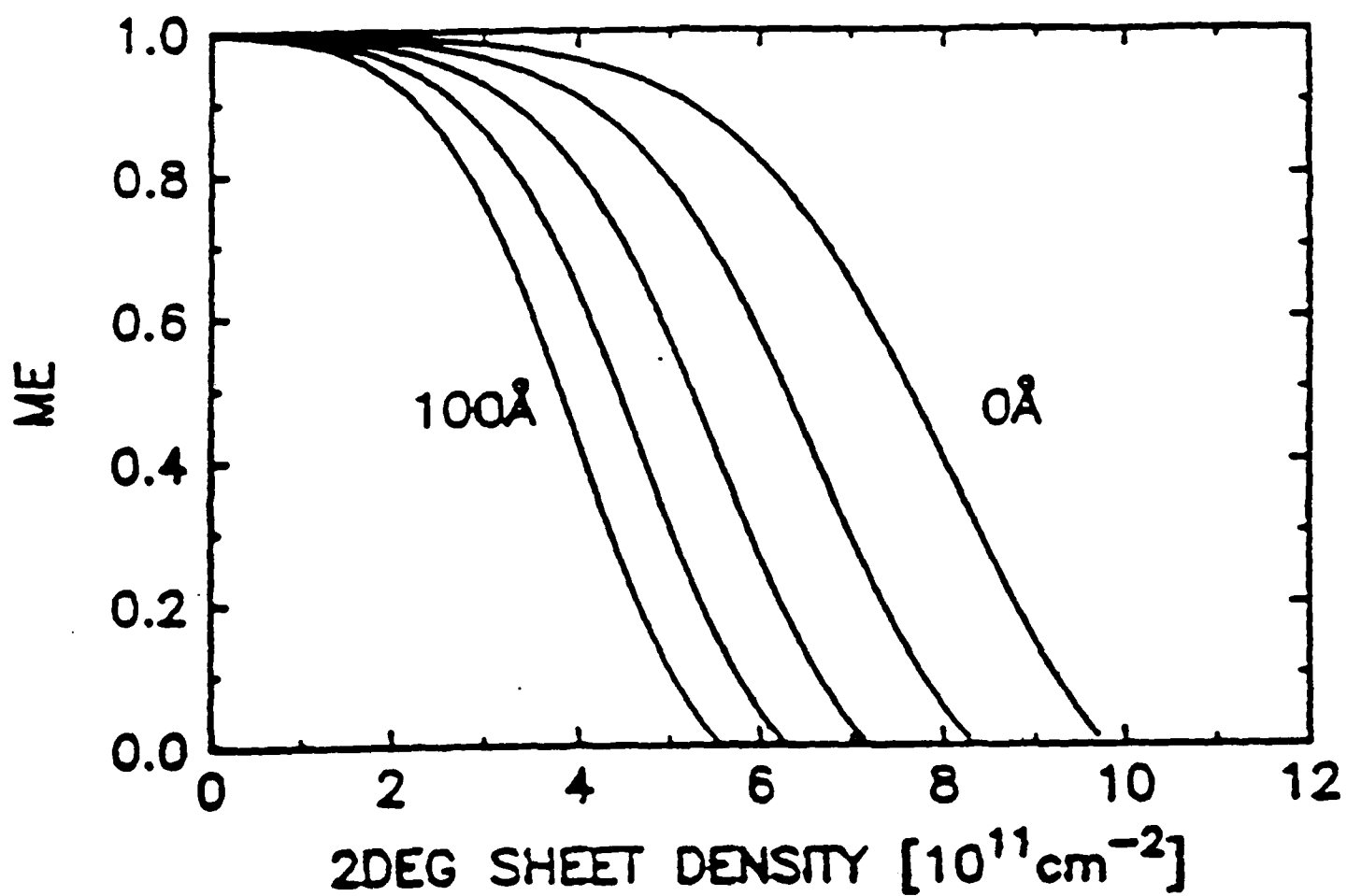


Figure 2. 300 K ME vs. 2DEG sheet density is plotted for spacer thicknesses of 0, 25, 50, 75, and 100 Å.

### **TASK 3    *MBE GROWN-LATTICE-MATCHED HETEROJUNCTION FOR IMPROVED TRANSISTORS***

L.F. Eastman and G.W. Wicks

#### **OBJECTIVE**

The objective of this task is the continued investigation and improvement of heterojunction structures for transistor applications. Two particular structures, the modulation doped field effect transistor (MODFET) and the heterojunction bipolar transistor (HBT) were studied.

#### **DISCUSSION OF STATE-OF-THE-ART**

There were two general types of investigations made in this task. The first type is a materials study of effects during MBE growth which cause the resulting structure to be different from that which was intended. Examples of this type of study are dopant diffusion in HBT's which degrade emitter injection efficiency and roughening of interfaces in quantum well MODFET's which cause degraded and anisotropic electron mobilities. The second type of study made in this task is an engineering of the heterostructure to optimize the desired characteristics of electrons or holes. Examples of this type of study are insertion of a tunnel barrier at the emitter-base junction of an HBT to improve injection efficiency, and use of an  $\text{Al}_x\text{Ga}_{1-x}\text{As}$  spacer layer with  $x = 45\%$  to obtain the maximum conduction band discontinuity.

#### **PROGRESS**

##### **Bipolar Transistors**

1. An optical technique was developed to directly measure the injection efficiency,  $\gamma$ , of an HBT. Measured  $\gamma$ 's on original device structures were 30-40% instead of the theoretical 98-99%. This degradation in  $\gamma$  was found to be caused by diffusion of Be from the GaAs base into the AlGaAs emitter. Insertion of a 200 Å undoped GaAs setback layer at the emitter-base junction was found to restore  $\gamma$  to theoretical values. Be diffusion in GaAs was thoroughly studied and found to occur by substitutional-interstitial diffusion for lower doping concentration ( $N_{\text{Be}} > 10^{19}\text{cm}^{-3}$ ,  $D \approx 10^{-9}\text{cm}^2/\text{s}$ ).
2. The concept was developed that an appropriately designed tunnel barrier placed at the emitter-base junction of a bipolar transistor could have a near unity transmission coefficient for electrons but a very small transmission coefficient for holes, thereby enhancing the electron injection efficiency,  $\gamma$ , and current gain,  $\beta$ . The concept was tested on a GaAs homojunction npn transistor, but the concept is equally applicable to HBT's. In this experiment the reference homojunction transistor had a low  $\beta$  of  $\sim 8$ , as expected. Insertion of a low tunnel barrier (consisting of  $\text{Al}_{0.45}\text{Ga}_{0.55}\text{As}$ ) or a narrow ( $\ell_b = 20$  Å) barrier had very little effect. However when a higher (AlAs) and wider ( $\ell_b = 50$  Å) tunnel barrier was inserted at the emitter base junction,  $\beta$  rose to  $\sim 250$ . This value was comparable to a reference HBT.

## MODFET's

Conventional AlGaAs/GaAs MODFET structures utilize  $\text{Al}_x\text{Ga}_{1-x}\text{As}$  with  $x = 30\%$  for both the electron supplying layer and the undoped spacer. In some respects, it would be desirable to have lower  $x$   $\text{Al}_x\text{Ga}_{1-x}\text{As}$  in the electron supplying layer (to decrease DX centers) and higher  $x$   $\text{Al}_x\text{Ga}_{1-x}\text{As}$  in the spacer layer (to increase the barrier height which confines electrons to the two dimensional electron gas). For these reasons, MODFET structures with  $\text{Al}_{0.2}\text{Ga}_{0.8}\text{As}$  electron supplying layers and  $\text{Al}_{0.45}\text{Ga}_{0.55}\text{As}$  spacer layers were grown. They produced record conductivities for single two dimensional electron gases since high electron concentrations were maintained ( $n_{300\text{K}} \sim 1.0\text{--}1.2 \times 10^{12}\text{cm}^{-2}$ ) without degrading the mobility ( $\mu_{300\text{K}} \sim 100,000\text{--}120,000\text{cm}^2/\text{v-sec}$ ).

A variety of interesting effects relating to the inverted GaAs/AlGaAs interface were discovered in modulation doped quantum wells. Anisotropic conductivity was detected, with the maximum conductivity along the [110] direction and the minimum along the  $[\bar{1}10]$  direction. These anisotropic effects are relaxed by a growth stop at the inverted interface, higher growth temperatures, use of superlattice buffer layers, increasing the thickness of the quantum well and increasing the sheet concentration of the two dimensional electron gas. Also, higher and more isotropic mobilities result when substrates are misoriented approximately  $4^\circ$  off [001] toward [111]A.

## SCIENTIFIC IMPACT OF RESEARCH

The scientific impact of this research was improved understanding of the effects of the quality of the epitaxial material on device performance. Also, insight into the physics of the electron injection mechanisms in HBT's was gained.

## DEGREES

NONE

## JSEP PUBLICATIONS

1. "The Influence of V:III Flux Ratio on Unintentional Impurity Incorporation During Molecular Beam Epitaxial Growth", S.C. Palmateer, P.A. Maki, W. Katz, A.R. Calawa, J.C.M. Hwang and L.F. Eastman, Inst. Phys. Conf. Ser. No. 74, Chapter 3, 217-222 (1985).
2. "Electron Velocity vs. Electric Field in n-Type  $\text{Ga}_{0.47}\text{In}_{0.53}\text{As}$  Short Samples- Evidence for Ballistic Transport", T. Ohashi, M.I. Nathan, S.D. Mukherjee, G.W. Wicks, G. Rubino and L.F. Eastman, Inst. Phys. Ser. No. 74, Chapter 4, 293-297 (1985).
3. "Sub-Micrometer Quantum Well HEMT with  $\text{Al}_{0.3}\text{Ga}_{0.7}\text{As}$  Buffer Layer", L.H. Camnitz, P.A. Maki, P.J. Tasker and L.F. Eastman, Inst. Phys. Conf. Ser. No. 74, Chapter 5, 333-338 (1985).
4. "Optimized GaAs/(AlGa)As Modulation Doped Heterostructures", H. Lee, W.J. Schaff, G.W. Wicks, L.F. Eastman and A.R. Calawa, Inst. Phys. Conf. Ser. No. 74, Chapter 5, 321-326 (1985).

5. "The Effect of Doping on the Interface Between GaAs and AlGaAs", W.J. Schaff, P.A. Maki, L.F. Eastman, L. Rathbun, B. DeCooman and C.B. Carter, Proc. MRS, **37**, 15-21 (1985).
6. "Photoluminescence Determination of Well Depth of  $\text{Ga}_{0.47}\text{In}_{0.53}\text{As}/\text{Al}_{0.48}\text{In}_{0.52}\text{As}$  in an Ultrathin Single Quantum Well", K. Shum, P.P. Ho, R.R. Alfano, D.F. Welch, G.W. Wicks and L.F. Eastman, Physical Review B, **32** (6) 3806-3810 (Sept. 1985).
7. "Anomalous Redistribution of Beryllium in GaAs Grown by Molecular Beam Epitaxy", P. Enquist, G.W. Wicks and L.F. Eastman, J. Appl. Phys., **58** (11) 4130-4134 (Dec. 1985).
8. "Reflection High-Energy Electron Diffraction Intensity Oscillation Study of Ga Desorption from Molecular Beam Epitaxially Grown  $\text{Al}_x\text{Ga}_{1-x}\text{As}$ ", J. Ralston, G.W. Wicks and L.F. Eastman, J. Vac. Sci. Technol., **B4** (2) 594-597 (March/April 1986).
9. "DC and RF Characterization of a Planar-Doped Double Heterojunction MODFET", Y-K. Chen, D.C. Radulescu, P.J. Tasker, G.W. Wang and L.F. Eastman, Inst. Phys. Conf. Ser., **83**, Chapter 8, 581-586 (1987).
10. "Anisotropic Transport in Modulation-Doped Quantum-Well Structures", D.C. Radulescu, G.W. Wicks, W.J. Schaff, A.R. Calawa and L.F. Eastman, J. Appl. Phys., **61** (6) 2301-2306 (March 1987).

## **TASK 4    *HIGH SPEED AMPLITUDE MODULATION OF SEMICONDUCTOR LASERS AND LIGHT EMITTING DIODES***

L.F. Eastman and G.W. Wicks

### **OBJECTIVE**

The objective of this task is to investigate mechanisms which could be utilized in opto-electronic devices to produce optical signals which can be modulated at high frequencies.

### **DISCUSSION OF STATE-OF-THE-ART**

There are two main areas of investigation in this task: effects of electric fields on the optical properties of quantum wells and disordering of superlattices via impurity implantation or diffusion. In both cases, applications of these effects to high speed light emitters or optical modulators was emphasized.

### **PROGRESS**

1. A gated quantum well LED was fabricated. A gate voltage creates an electric field perpendicular to the quantum well interfaces which separates the holes and electrons, thereby quenching the optical output. Modulation speed in this device should be limited by the transit time of electrons and holes to opposite sides of the quantum wells and by RC time constants, both of which are much faster than the carrier lifetime which limits conventional LED's. This particular gated LED requires 3-5 volts of gate bias to cause a 75% reduction in output intensity.
2. Modulation of (room temperature) exciton-related absorptive and refractive properties of GaAs/AlGaAs MQW waveguide structures has direct application to a number of novel structures for high speed photonic switching. Ionization of excitons via an electric field applied in the plane of the QW's is particularly attractive for very high speed optical waveguide modulators because coplanar stripline electrodes can be utilized to apply the necessary high frequency bias signals.

After depositing interdigitated Ti:Au contacts (20 micron fingers, 20 micron spaces, total area = 3 mm<sup>2</sup>), photocurrent measurements have been made with a broadband optical source to study the change in optical absorption as a function of applied electric field in a GaAs/AlGaAs MQW waveguide structure. In the structure studied, an applied lateral electric field of  $\sim 1.5 \times 10^4$  V/cm was sufficient to essentially annihilate the excitonic peaks in the band edge absorption profile (as measured by photocurrent). In a coplanar stripline modulation structure with 5 micron electrode spacing, the above field corresponds to a bias of 7.5 V. Research is continuing to apply the above effect to a reactive modulator consisting of a MQW waveguide with a 2nd order distributed feedback (DFB) grating corrugated in the surface.

3. We have demonstrated substantial increases in the energies of room temperature exciton transitions in GaAs/AlGaAs superlattices which have been partially intermixed via the impurity-free vacancy diffusion process. In the samples studied, the above process allows continuously variable energy shifts of at least 60 meV while still maintaining clearly resolved exciton resonances.

The superlattice samples consisted of 25 periods of 80 Å GaAs layers alternating with 80 Å  $\text{Al}_{0.3}\text{Ga}_{0.7}\text{As}$  layers (total thickness 4000 Å) grown by molecular beam epitaxy. Localized intermixing of the layered structure was accomplished by selective deposition of a  $\text{SiO}_2$  capping layer followed by rapid thermal annealing (RTA) at temperatures between 850° and 950°C for 15 sec. As previously reported [1], intermixing is attributed to a large diffusion rate of Ga into the  $\text{SiO}_2$ , accompanied by Ga vacancy diffusion into the superlattice.

The degree of intermixing was characterized using Raman spectroscopy and room temperature photoluminescence. Shifting and broadening of the exciton transitions were studied using photocurrent (PC) spectroscopy and electroreflectance.

Regions not capped with  $\text{SiO}_2$  demonstrated negligible thermal intermixing due to RTA alone over the entire temperature range studied, while also exhibiting well-resolved heavy hole (hh) and light hole (lh) transitions.

In contrast, for the  $\text{SiO}_2$  capped regions the degree of intermixing varied from slight (850°C) to extensive, but not complete (950°C). After RTA the exciton transitions were broadened and shifted to higher energies in all cases, which can be attributed to compositional grading at the quantum well barrier interface. Measured shifts in exciton peak energies varied from 3.5 meV (850°C) to 60 meV (950°C). Both heavy hole and light hole exciton peaks remained resolved in PC spectra for shifts as large as 30 meV. A single broad exciton peak is observed following the 950° anneal. The above shifted and broadened excitons transitions have also been observed in electroreflectance spectra.

This is the first reported study of excitonic behavior during the selective intermixing of semiconductor superlattices. The ability to continuously change the effective bandgap while maintaining the exciton absorption and refractive properties of the superlattice may have a variety of optical device applications, several of which we are currently exploring.

## REFERENCES

1. D.G. Deppe, L.J. Guido, N. Holonyak Jr., K.C. Hsieh, R.D. Burnham, R.L. Thornton and T.L. Paoli, Appl. Phys. Lett., **49**, 510 (1986).

## SCIENTIFIC IMPACT OF RESEARCH

The scientific impact of this task is an improved understanding of the behavior of excitons in quantum wells under applied electric fields. It was demonstrated that field ionization of excitons can be utilized to modulate the output of light emitting devices. Additional characteristics of excitons in multi quantum well structures were measured which will provide useful information for the construction of ultra high speed optical modulators

## DEGREES

1. E. Elias, M.S. (Aug. 1985)  
"A Gate Modulated Quantum Well Light Emitting Diode"

2. E.A. VanGieson, M.S. (Jan. 1985)  
"High Quality Multiple AlGaAs/GaAs Quantum Well and Graded Refractive Index Separate Confinement Heterostructure Quantum Well Lasers Grown Via Molecular Beam Epitaxy"

#### JSEP PUBLICATIONS

1. "Exciton Transport in Optically Excited  $\text{Al}_x\text{Ga}_{1-x}\text{As}$ -GaAs Single Quantum Well", H.Q. Le, B. Lax, P.A. Maki, S.C. Palmateer and L.F. Eastman, J. Appl. Phys., **55** (12) 4367-4372 (June 1984).
2. "The Structure of Ion Implanted  $\text{Al}_x\text{Ga}_{1-x}\text{As}$ /GaAs Superlattices", B.C. DeCooman, S.H. Chen, C.B. Carter, J. Ralston and G.W. Wicks, Inst. Phys. Conf. Ser., **76**, Section 7 (1985).
3. "Defect Structure and Intermixing of Ion-Implanted  $\text{Al}_x\text{Ga}_{1-x}\text{As}$ /GaAs Superlattices", J. Ralston, G.W. Wicks, L.F. Eastman, B.C. DeCooman and C.B. Carter, J. Appl. Phys., **59** (1) 120-123 (Jan. 1986).
4. "GaAs/AlGaAs Waveguide with Grating Coupler Fabricated by Selective Superlattice Intermixing", J.D. Ralston, L.H. Camnitz, G.W. Wicks and L.F. Eastman, Inst. Phys. Conf. Ser., **83**, 367-372 (1987).

## **TASK 5    *HIGH SPEED RECEIVERS FOR OPTICAL COMMUNICATIONS***

J.M. Ballantyne

### **OBJECTIVE**

To develop large area detectors suitable for use in monolithically integrated photoreceivers, and to develop MOCVD growth techniques of materials suitable for monolithic optoelectronic subsystems.

### **DISCUSSION OF STATE-OF-THE-ART**

#### **PHOTORECEIVERS**

Several easily integrable photoreceivers (e.g. [1-4]) have been reported on recently. Some typical performance figures are 112 V/W responsivity at 1.5 GHz [3] and 400 V/W responsivity at 2 GHz [4].

#### **MOCVD GROWTH**

MOCVD growth has developed greatly over the past five years, and techniques have been developed in many laboratories for growing layers in a variety of compositions, of higher purity, and with thin layers and abrupt interfaces to rival MBE. Our work has been leading in the production of high purity, high quality layers in GaInAsP compounds suitable for optoelectronics. The performance of lasers and detectors is a severe test of material quality, and has been a continuing method used in our work to evaluate materials. Transverse-junction-stripe (TJS) lasers are a particularly demanding device, since they are very sensitive to current leakage at interfaces. We have completed a major study of such lasers using In in the active layer.

Many TJS lasers, fabricated in the GaAs/AlGaAs material system, have been reported [8,9,10]. The GaAs/AlGaAs TJS lasers have threshold currents as low as 12 mA, and demonstrate good lateral mode stability [10]. Furthermore, many high quality lasers of other geometries have been reported which have GaInAs or GaInAsP active regions [11,12,13]. No high-quality TJS lasers, however, have been demonstrated in any material system other than GaAs/AlGaAs. The two reported attempts at long-wavelength TJS devices were done in the InP/GaInAsP material system, resulting in emission wavelengths near 1.15 micron. TJS lasing was only achieved with pulsed operation at cryogenic temperatures (100 mA threshold current at 100°K) [14], or with extremely high threshold currents (250 mA at 287°K) [15]. This poor performance was attributed to current leakage through the n<sup>+</sup> substrate.

### **PROGRESS**

#### **PHOTORECEIVERS**

A monolithic photoreceiver was designed and realized [5]. It has a 3200 V/W responsivity at 1 GHz. The photocurrent gain is 200, which when coupled with the 1 GHz 3 db frequency gives a 200 GHz gain-bandwidth product. The receiver performs as above while driving a 50 ohm load to 1 volt peaks. The receiver utilizes an integrated photodiode, one of three types of detectors studied that are trivial to integrate in GaAs E/D ion-implanted MESFET processes. The relative merits of an



easily integrated photoconductor and two types of easily integrable photodiodes were studied. These detectors require absolutely no process changes or additions to the MESFET process [6]. The photoconductor has a high gain (27) and moderate speed (3 db at 250 MHz), while the photodiodes are faster, with the one utilized in the photoreceiver having a FWHM  $< 50$  ps, a 3 db point over 5 GHz and a gain of 0.2 (quantum efficiency 20%). The impedance properties of the photoconductor were examined to successfully explain the photoconductor output signal, which deviated from the simple theory by showing larger than expected signals. An interesting operating point of the detector was observed where the device reactance was eliminated over a wide frequency range, so that RC and LR time delays are not observed [7].

### MOCVD GROWTH

Epitaxial layers intended for use in semiconductor lasers were grown by low-pressure metalorganic chemical vapor deposition. Three types of layers were grown, and the quality of the material was evaluated by fabricating lasers from each layer. The first type was grown on semi-insulating InP substrates, and consisted of a double heterostructure with a 0.2 micron GaInAs active region surrounded by 1.5 micron InP cladding regions. Transverse junction stripe (TJS) lasers were fabricated from this material. Both the second and third types of layers were grown on  $n^+$  doped GaAs substrates. The second type of layer was a graded-index separate confinement heterostructure (GRIN SCH) with 0.4 micron thick AlGaAs graded regions surrounding a 150 Å thick GaAs quantum well. For this structure the Al content ranged from 20 to 60%. The third type was also a GRIN SCH, but it had a strained GaInAs, rather than an unstrained GaAs, quantum well. For the strained structure the Al content ranged from 0 to 40%. Broad area and ridge waveguide lasers were fabricated from both types of GRIN SCH layers.

The TJS devices reported here used semi-insulating substrates, and had both contacts deposited on the top, in an attempt to avoid the previously-reported current leakage problem. Despite this precaution, the TJS devices, which were fabricated from the double-heterostructure material, did not lase at room temperature. Through careful evaluation of the devices' electroluminescence emission, it was determined that this was at least partially due to the particular doping densities used in the epitaxial layer, which resulted in significant amounts of leakage current flowing through one of the InP cladding layers. The devices did, however, lase at temperatures below 160°K, and had threshold currents of 15 to 45 mA at 77°K, with emission wavelengths near 1.6 micron.

We have thus demonstrated the first TJS lasers to operate at a wavelength greater than 1.2 micron. The use of a semi-insulating substrate was intended to eliminate previously-reported current leakage problems; leakage through one of the cladding layers, however, lessened the advantage of this design. The use of low doping levels in the cladding regions should eliminate this problem.

The use of strained epitaxial layers in lasers is interesting because it is the only means of tailoring the emission wavelength of lasers fabricated in ternary material systems other than GaAs-AlGaAs. For the devices reported here, the use of a single strained GaInAs quantum well, rather than an unstrained GaAs well, results in an emission wavelength of 1.6 micron, rather than 840 nm. Previous attempts at strained-layer lasers, however, have resulted in quite short-lived devices [16,17,18]. Thus material quality and stability, and the related issue of device lifetime, are key with respect to the use of strained layers in practical devices.

The broad-area strained-layer lasers associated with the present work exhibited one of the lowest threshold current densities ever reported for any injection laser:  $152 \text{ A/cm}^2$  [19]. This is a very strong indication that these epitaxial layers are of unusually high quality.

The strained-layer ridge waveguide lasers emitted near 1 micron; the ridge waveguide was fabricated by chemically-assisted ion beam etching. The lasers had threshold currents near 17 mA with fundamental lateral mode operation to five times this value. The first reported strained-layer current-injection lasers to run cw at room temperature, they operated, without bonding, to greater than 24 mW/facet (100 mADC), and had 18 mW/facet (80 mADC) lifetimes in excess of 144 hours [20]. Although differing test conditions make the results difficult to compare accurately, this seems to be at least a factor of 100 better lifetime performance than has been previously reported for any strained-layer laser [18].

## SCIENTIFIC IMPACT OF RESEARCH

### PHOTORECEIVERS

The photoreceiver and detectors studied in this work are interesting since the detectors use only those processing steps already available for the MESFETs in the receiver circuitry. The photodetectors can be included in a computer aided design (CAD) library as "cells" in exactly the same manner as the MESFETs, resistors, capacitors, etc. already available in the process. The circuit designer can then be a step closer to designing photoreceiver circuitry by using standard photodetector "cells" without having to worry excessively about acquiring great expertise in photodetector technology. He or she can look at the device as a characterized "black box" with only the most rudimentary knowledge of its operation, in much the same way as many silicon VLSI designers use MOSFETs with only some feel for the first order approximations of the device physics, while many second order effects can be ignored in most designs.

The interesting zero-reactance point observed in the photoconductor is potentially useful in speeding up other photodetectors if the speed limitation is due to circuit effects (e.g. RC delay times) and the detector is not already transit time limited. If the detector is designed such that its intrinsic inductance and capacitance satisfy a certain condition explained in [7], then the circuit effects are negligible and the detector will only be limited by carrier transit times.

### MOCVD GROWTH

A variety of MOCVD layers were grown in the 3-year period, including heterostructures and quantum wells in three systems: AlGaAs/GaAs; GaInAs/InP; and AlGaAs/GaInAs/GaAs. In the first year we set the MOCVD state-of-the-art in the first two systems, and have now applied this technology to produce detectors and lasers. We have completed groundbreaking work in GaInAs/GaAs homomorphic layers for lasers which yielded threshold current density of  $150 \text{ A/cm}^2$ . We have made lasers from the AlGaAs/GaAs material with thresholds of 9 mA which are suitable for monolithic integration. We have also made high quality, high power single mode AlGaAs/GaAs laser diode arrays from this material. The most significant aspects of the laser work are:

- 1) The demonstration of an entirely new homomorphic materials structure which produces reliable lasers at 1 micron on GaAs. This materials structure is very significant for integrated optics (the substrate is transparent and the absorbing structure may be eraseable), for high power semiconductor lasers, and perhaps as a replacement for YAG lasers in communications systems.
- 2) The demonstration of MOCVD growth and device fabrication techniques using reactive ion beam etching to produce reliable, manufacturable, low loss optical devices with extreme repeatability.

Overall, the materials and device results show that the MOCVD approach is exceeding versatile and successful for producing materials for integrated optoelectronics.

### DEGREES

1. Glen Feak, Ph.D., August 1987
2. Steve Fischer, Ph.D., May 1987
3. Steve Wojtczuk, Ph.D., May 1987
4. Jimmie Lee Russell, Ph.D., May 1987
5. Kam Tai Chan, Ph.D., August 1986
6. G. Sonek, Ph.D., August 1986
7. Ruby Nandini Ghosh, M.S., January 1986

### REFERENCES

1. "A Monolithic Four-Channel Photoreceiver Integrated on a GaAs Substrate Using Metal-Semiconductor-Metal Photodiodes and FET's", M. Makiuchi, H. Hamaguchi, T. Kumai, M. Ito, O. Wada and T. Sakurai, IEEE Elec. Dev. Lett., EDL-6, 634-635 (1985).
2. "Planar Monolithic Integration of a GaAs Photoconductor and a GaAs FET", D. Decoster, J.P. Vilcot, M. Constant, J. Ramdani, H. Verrielle and J. Vanbremeersch, Elec. Lett., 22, 193-195 (1986).
3. "Monolithic GaAs Photoreceiver for High-Speed Signal Processing Applications", W.S. Lee, G.R. Adams, J. Mun and J. Smith, Elec. Lett., 22, 147-148 (1986).
4. "GaAs Optoelectronic Integrated Receiver with High-Output Fast-Response Characteristics", H. Hamaguchi, M. Makiuchi, T. Kumai and O. Wada, IEEE Elec. Dev. Lett., EDL-8, 39-41 (1987).
5. "Monolithically Integrated Photoreceiver with Large Gain-Bandwidth Product", S.J. Wojtczuk, J.M. Ballantyne, Y.K. Chen and S. Wanuga, to be published in Elec. Lett. (1987).
6. "Comparative Study of Easily Integrable Photodetectors", S.J. Wojtczuk, J.M. Ballantyne, S. Wanuga and Y.K. Chen, to be published in IEEE J. Lightwave Tech. (1987).

7. "Impedance Properties and Broad-Band Operation of GaAs Photoconductive Detectors", S.J. Wojtczuk and J.M. Ballantyne, IEEE J. Lightwave Tech., LT-5, 320-324 (1987).
8. "Long-Life GaAs-GaAlAs TJS Laser with Low Threshold Current and Fundamental Transverse and Single Longitudinal Mode", H. Namizaki, M. Ishii, H. Kan, E. Ohmura, R. Hirano and A. Ito, Optics Comm., 18, p. 39 (1976).
9. "15 mW Single Mode CW Operation of Crank Structure TJS Laser Diodes at High Temperature", H. Kumabe, T. Tanaka, S. Nita, Y. Seiwa, T. Sogo and S. Takamiya, Jap. J. Appl. Phys., 21 (1) 347-351 (1982).
10. "High Temperature Single Mode CW Operation with a TJS Laser using a Semi-Insulating GaAs Substrate", H. Kumabe, T. Tanaka, H. Namizaki, S. Takamiya, M. Ishii and W. Susaki, Jap. J. Appl. Phys., 18 (1) 371-375 (1979).
11. "1.5 Micron Region InP/GaInAsP Buried Heterostructure Lasers on Semi-Insulating Substrates", T. Matsuoka, K. Takahei, Y. Noguchi and H. Nagai, Elec. Lett., 17, 12-14 (Jan. 1981).
12. "Low Threshold Current CW Operation of InP/GaInAs Buried Heterostructure Lasers", Y. Noguchi, K. Takahei, Y. Suzuki and H. Nagai, Jap. J. Appl. Phys., 19, L759-L762 (Dec. 1980).
13. "MBE-Grown InGaAs/InP BH Lasers with LPE Burying Layers", Y. Kawamura, Y. Noguchi, H. Asahi and H. Nagai, Elec. Lett., 18, 91-92 (Jan. 1982).
14. "Oxide Defined TJS Lasers in InGaAsP/InP DH Structures", D.J. Bull, N.B. Patel, F.C. Prince and Y. Nannichi, IEEE J. Quantum Elec., QE-15, 710-713 (Aug. 1979).
15. "Dual Wavelength InGaAsP/InP TJS Lasers", S. Sakai, T. Aoki and M. Umeno, Elec. Lett., 18, 18-20 (Jan. 1982).
16. "Continuous 300-K Laser Operation of Strained Superlattices", M.J. Ludowise, W.T. Dietze, C.R. Lewis, M.D. Camras, N. Holonyak, Jr., B.K. Fuller and M.A. Nixon, Appl. Phys. Lett., 42, 487-489 (March 1983).
17. "Stimulated Emission in Strained-Layer Quantum-Well Heterostructures", M.D. Camras, J.M. Brown, n. Holonyak, Jr., M.A. Nixon, R.W. Kaliski, M.J. Ludowise, W.T. Dietze and C.R. Lewis, J. Appl. Phys., 54, 6183-6189 (Nov. 1983).
18. "Strained-Layer Quantum-Well Injection Laser", W.D. Laidig, P.J. Caldwell, Y.F. Lin and C.K. Peng, Appl. Phys. Lett., 44, 653-655 (April 1984).
19. "Graded Index Separate-Confinement InGaAs/GaAs Strained-Layer Quantum-Well-Laser Grown by Metalorganic-Chemical Vapor Deposition", D. Fekete, K.T. Chan, J.M. Ballantyne and L.F. Eastman, Appl. Phys. Lett., 49, 1659-1660 (Dec. 1986).
20. "Ridge Waveguide Injection Laser with a GaInAs Strained-Layer Quantum Well ( $\lambda = 1 \mu\text{m}$ )", S.E. Fischer, D. Fekete, G.B. Feak and J.M. Ballantyne, Appl. Phys. Lett., 50, 714-716 (March 1987).

### JSEP PUBLICATIONS

1. "A Photoluminescence Study of the Growth of InP by Metalorganic Chemical Vapor Deposition", L.D. Zhu, K.T. Chan, D.K. Wagner and J.M. Ballantyne, J. Appl. Phys., **57**, 5486 (1985).
2. "Growth of High Quality GaInAs on InP Buffer Layers by Metalorganic Chemical Vapor Deposition", K.T. Chan, L.D. Zhu and J.M. Ballantyne, Appl. Phys. Lett., **47**, 44 (1985).
3. "Very High Mobility InP Grown by Low Pressure Metalorganic Vapor Phase Epitaxy Using Solid Trimethylindium Source", L.D. Zhu, K.T. Chan and J.M. Ballantyne, Appl. Phys. Lett., **47**, 47 (1985).
4. "MOCVD Growth and Characterization of High Quality InP", L.D. Zhu, K.T. Chan and J.M. Ballantyne, J. Crystal Growth (1985).
5. "Two-Dimensional Electron Gas in InGaAs/InP Heterojunctions Grown by Atmospheric Pressure Metalorganic Chemical Vapor Deposition", L.D. Zhu, P.E. Sulewski, K.T. Chan, K. Muro, J.M. Ballantyne and A.J. Sievers, J. Appl. Phys., **58**, 3145 (1985).
6. "Epitaxial Growth and Characterization of Indian Phosphide and Gallium Indian Arsenide by Metalorganic Chemical Vapor Deposition", K.T. Chan, Ph.D. Thesis, Cornell University (Aug. 1986).
7. "Optimized Interdigitated Contact Design", S.J. Wojtczuk and J.M. Ballantyne, Cornell University, Internal Report (1986).
8. "Low Threshold Ridge Waveguide Single Quantum Well Laser Processed by Chemically-Assisted Ion Beam Etching", L.D. Zhu, G.B. Feak, R.J. Davis, J.M. Ballantyne and D.K. Wagner, IEEE J. Quant. Elec., **QE-23**, 309 (1987).
9. "In-Phase Coupling Between Ridge Guide Lasers by Introducing Distributed Saturable Absorption Regions in Subordinate Laser Cavities", L.D. Zhu, G.B. Feak and J.M. Ballantyne, Appl. Phys. Lett., **50** (22) (1987).
10. "Monolithic Integration of GaAs Light-Emitting Diodes and Si Metal-Oxide Semiconductor Field-Effect Transistors", R.N. Ghosh, B. Griffing and J.M. Ballantyne, Appl. Phys. Lett., **48**, 370 (1986).
11. "Monolithically Integrated Photoreceiver With Large Gain-Bandwidth Product", S.J. Wojtczuk, J.M. Ballantyne, Y.K. Chen and S. Wanuga, Elec. Lett., **23**, 574 (1987).
12. "Comparative Study of Easily Integrable Photodetectors", S.J. Wojtczuk, J.M. Ballantyne, S. Wanuga and Y.K. Chen, to be published in IEEE J. Lightwave Tech. (1987).
13. "Impedance Properties and Broad-Band Operation of GaAs Photoconductive Detectors", S.J. Wojtczuk and J.M. Ballantyne, IEEE J. Lightwave Tech., **LT-5**, 320-324 (1987).

14. "Graded Index Separate-Confinement InGaAs/GaAs Strained-Layer Quantum-Well-Laser Grown by Metalorganic-Chemical Vapor Deposition", D. Fekete, K.T. Chan, J.M. Ballantyne and L.F. Eastman, Appl. Phys. Lett., 49, 1659-1660 (Dec. 1986).
15. "Ridge Waveguide Injection Laser with a GaInAs Strained-Layer Quantum Well ( $\lambda = 1 \mu\text{m}$ )", S.E. Fischer, D. Fekete, G.B. Feak and J.M. Ballantyne, Appl. Phys. Lett., 50, 714-716 (March 1987).
16. "GaAs/GaAlAs Quantum Well Laser with a Laterally Spatial Variation in Thickness Grown by Metalorganic-Chemical Vapor Deposition", D. Fekete, D. Bour, J.M. Ballantyne and L.F. Eastman, Appl. Phys. Lett., 50 (11) 635 (1987).
17. "Monolithically Integrable High Speed Photodetectors", S.J. Wojtczuk, Ph.D. Thesis, Cornell University (1987).
18. "Low Threshold ridge Waveguide Single Quantum Well Lasers", G.B. Feak, Ph.D. Thesis, Cornell University (1987).
19. "Semiconductor Lasers with Gallium Indium Arsenide Active Regions for Monolithic Optoelectronics", S.E. Fischer, Ph.D. Thesis, Cornell University (1987).

## **TASK 6 SPECTRAL AND DYNAMIC CHARACTERISTICS OF SEMICONDUCTOR MATERIALS AND STRUCTURES**

C.L. Tang

### **OBJECTIVE**

The main objective of this program is to investigate the dynamics of hot carriers in III-V compounds and quantum wells. The results are important to the development of high speed electronic and opto-electronic devices which make use of hot electrons in semiconductors.

### **DISCUSSION OF STATE-OF-THE-ART**

Of particular current interest in the development of ultra-fast electronic and opto-electronic devices are ballistic transport and quantum interference effects in semiconductors and quantum well and superlattice structures. There are two basic approaches to the study of these problems. In the first approach, the emphasis is on the transport properties of the carriers. In structures such as the so called tunneling hot electron transfer amplifier (THETA devices), electrons are injected into a drift region on the order of the mean-free path or shorter and then collected. The relaxation or transport properties of the injected carriers in the drift region are usually inferred from the measured properties of the overall structure including the injection, drift, and collection regions. This requires a detailed knowledge of the injection and collection processes which can complicate the interpretation of the data. In the second approach, nonequilibrium carriers are created in a volume with linear dimensions much larger than the mean-free path. Carrier dynamics are determined through time-dependent measurements using femtosecond lasers. The spatial and time-domain measurements complement each other. At the present time, the accuracy in time-domain measurements of carrier dynamics is much the better of the two.

The ultimate speed of transit time electronic devices is limited by the intraband relaxation time of nonequilibrium carriers in the drift region of the device. Thus, a clear understanding of the relaxation dynamics of such carriers is vital to our overall goal of pushing the limiting speed of transit time devices into the subpicosecond time domain.

There are two basic approaches in time-domain studies of the relaxation processes in semiconductors using femtosecond lasers. One is to use high-repetition rate (10<sup>8</sup>Hz) systems which typically have the pulse width of 40 fs. The other approach is to use pulse-compression systems external to the laser and achieve shorter pulse width (approximately 10 fs) at the expense of repetition rate (down typically by 4 to 5 orders of magnitude). The high-repetition rate is crucial to achieving the signal-to-noise ratio needed to give reliable quantitative results. Since the relaxation dynamics in III-V compounds are more or less understood qualitatively based upon earlier extensive indirect results obtained in transport studies in connection with electronic device research, if anything is to be gained by optical studies, it is important that the optical studies give accurate quantitative results. Thus, we have opted for the high-repetition system at the expense of ultimate time resolution. Since the carrier concentration range of interest the fastest process is approximately 40 fs and our high-repetition system can resolve any process down to 25 fs, there is nothing to be gained for our experiments by using pulse-compression schemes to shorten the laser pulse width at a drastically reduced

pulse repetition rate. The optical correlation-spectroscopic technique based upon high-repetition femtosecond lasers has been extensively developed at Cornell and we plan to continue to use this approach.

There have recently been a number of studies reported on the use of femtosecond lasers to study the relaxation dynamics of hot carrier in semiconductors. Except for our recent work, all the results reported are qualitative. Our recent work gives specific numerical results on the rates of various scattering processes. These are discussed briefly in the following section and in detail in our publications listed at the end of this progress report.

## PROGRESS

Our efforts during the past three years have been devoted to developing and improving the optical-correlation technique for measuring ultrafast processes in various optical materials and in applying the technique to the study of relaxation dynamics of hot carriers in compound semiconductors and related structures.

The process that our high repetition-rate system can resolve has been steadily faster, from approximately 80 fs to 25 fs. The time resolution for slower processes is now down to a few femtoseconds. This is due in part to the improvements made in our laser system and signal-processing technique and in part due to the signal analysis procedure developed in our laboratory. The problem of extracting accurate relaxation rates from the data in our experiments is complicated by the fact that the carrier decay is usually governed by several relaxation processes. The rates of these processes range from less than 40 fs to several picoseconds, and several processes of comparable rates contribute simultaneously to the 40 fs decay component, for example. To sort out the various exponential components from a single measured decay curve and to determine the rates for the individual processes require very accurate experimental data and a reliable data analysis procedure.

A powerful procedure based upon the principle of linear-prediction has been developed for the quantitative analysis of optical-correlation and pump-probe types of experiments. It is capable of extracting multiple exponential or exponentially damped sinusoidal components from noisy data. Furthermore, it can be used to analyze data which is not simply the response of the system being studied, but rather the convolution of a non-negligible instrument function with the desired response. It can be used to deduce time constants which are considerably shorter than the laser pulse itself. This procedure is used extensively in the analysis of our data.

Experimentally, the relaxation dynamics of nonequilibrium carriers in GaAs and related compounds immediately following femtosecond photo-excitation have been studied extensively in recent years. While the experimental results at room temperature are fairly well established, much work remains to determine the physical origins of various observed femtosecond decay processes. We have recently carried out an extensive study of the relaxation dynamics of such carriers at cryogenic temperatures down to 10°K. By scanning the temperature, the position of the initially photo-excited state can be scanned continuously from above the satellite valley minima (L and X valleys) to less than one LO-phonon above the  $\Gamma$ -valley minimum. By eliminating selectively the possibility of different scattering processes as the temperature is scanned, it is possible to identify unambiguously the physical origins of the exponential components observed in the initial relaxation decay from the photo-excited states.



In our earlier room temperature experiments on GaAs and  $\text{Al}_{0.32}\text{Ga}_{0.68}\text{As}$ , the initial relaxation of the photoexcited carriers was found to contain two sub-picosecond exponential components with time constants of approximately 40 fs and 160 fs. The 40 fs component was attributed to  $\Gamma$ -L valley scattering with possible contributions from carrier-carrier scattering. However, the relative contribution of the two was uncertain. The 160 fs component was attributed to polar-optical-phonon scattering within the central valley based on comparisons with calculated results.

Our new results obtained by scanning the temperature of  $\text{Al}_{0.35}\text{Ga}_{0.65}\text{As}$  samples at carrier densities in the range from  $10^{16}$  to  $10^{18}\text{cm}^{-3}$  confirm and clarify these conclusions. More specifically, it is found that as the initial photo-excited state falls below the X- and  $\Gamma$ -valley minima, the relative amplitude of the 40 fs component drops by a factor of approximately 2.5 to 3 depending on the carrier density and the sample temperature, but the time constant does not change significantly. This implies that at room temperature, the 40 fs component is mainly due to  $\Gamma$ -valley scattering with an approximately 20-15% contribution from carrier-carrier scattering, taking into account the fact that at low temperatures a significantly smaller fraction of the excited electrons can relax by emission of LO-phonons. The  $\Gamma$ -valley scattering rate is consistent with a deformation potential of  $10^9\text{eV/cm}$ . The rate due to carrier-carrier scattering also happens to be around  $(40\text{ fs})^{-1}$  at a carrier density of approximately  $10^{18}\text{cm}^{-3}$ . As the position of the initially excited state is scanned to less than one LO-phonon energy above the  $\Gamma$ -valley minimum, there is clear indication that the 160 fs component we observed was due to polar-optical-phonon scattering. Bailey, Stanton, and Hess have recently carried out an extensive ensemble Monte Carlo simulation of the femtosecond energy relaxation dynamics of nonequilibrium carriers in GaAs and related compounds. Their results show remarkable agreement with our conclusions based upon the femtosecond laser studies.

#### SCIENTIFIC IMPACT OF RESEARCH

The impact of our research is two-fold:

- (1) the information obtained on the relaxation dynamics of hot carriers in semiconductors is important to the understanding of the ultrafast processes in semiconductors and the development and improvement of ultrafast electronic and optoelectronic devices, and
- (2) the femtosecond laser technique developed for the experiments carried out should have a wide range of applications in the study of ultrafast processes in general and can be extended to other applications such as evaluating mm and sub-mm wave integrated circuit chips.

#### DEGREES

1. D.J. Erskine, Ph.D., Physics, June 1984  
"Ultrafast Relaxation Phenomenon of Photoexcited Carriers in GaAs and Related Compounds"
2. M.J. Rosker, Ph.D., Applied Physics, January 1987  
"Femtosecond Relaxation After Photoexcitation of Semiconductors and Large Dye Molecules"

## JSEP PUBLICATIONS

1. "Femtosecond Vibrational Relaxation of Large Organic Molecules", A.J. Taylor, D.J. Erskine and C.L. Tang, Chem. Phys. Lett., **103**, 430 (1984).
2. "Picosecond Relaxation of Hot Carriers in Highly Photoexcited Bulk GaAs and GaAs-AlGaAs Multiple Quantum Wells", Z.Y. Xu and C.L. Tang, Appl. Phys. Lett., **44**, 692 (1984).
3. "Stimulated Emission of GaAs/AlGaAs Multiple Quantum Well Structures Grown by MOCVD", Z.Y. Xu and C.L. Tang, Appl. Phys. Lett., **44**, 136 (1984).
4. "Femtosecond Studies of Intraband Relaxation in GaAs, AlGaAs and GaAs/AlGaAs Multiple Quantum Well Structures", D.J. Erskine, A.J. Taylor and C.L. Tang, Appl. Phys. Lett., **45**, 54-56 (1984).
5. "Femtosecond Studies of Intraband Relaxation of Semiconductors and Molecules", A.J. Taylor, D.J. Erskine and C.L. Tang, Proc. IV Topical Meet. on Ultrafast Phenomena, Monterey, CA (1984), Springer-Verlag (1985).
6. "Dynamic Burstein-Moss Shift in GaAs and GaAs/AlGaAs Multiple Quantum Wells", D.J. Erskine, A.J. Taylor and C.L. Tang, Appl. Phys. Lett., **45**, 1209-1211 (1984).
7. "Ultrafast Relaxation Dynamics of Photoexcited Carriers in GaAs and Related Compounds", A.J. Taylor, D.J. Erskine and C.L. Tang, J. Opt. Soc. Amer. B, **2**, 663-673 (April 1985).
8. "Femtosecond Relaxation Dynamics of Large Molecules", M.J. Rosker, F.W. Wise and C.L. Tang, Phys. Rev. Lett., **57**, 321-324 (1986).
9. "Intraband Relaxation Dynamics of Photoexcited Carriers in GaAs and Related Compounds", C.L. Tang, F.W. Wise and M.J. Rosker, Invited, Proc. 18th Int. Conf. on Solid State Devices and Materials, Tokyo, Japan, 157-159 (1986).
10. "Femtosecond Lasers and Ultrafast Processes in Semiconductors", C.L. Tang, in Nonlinear Optics: Materials and Devices, edited by Chr. Flytzanis and J.L. Oudar, Springer, Proceedings in Physics, **7**, Springer-Verlag, Berlin (1986).
11. "Femtosecond Optical Measurement of Hot Carrier Relaxation in GaAs, AlGaAs, and GaAs/AlGaAs Multiple Quantum Well Structures", M.J. Rosker, F.W. Wise and C.L. Tang, Appl. Phys. Lett. (Dec. 1986).
12. "Oscillatory Femtosecond Relaxation of Photoexcited Organic Molecules", F.W. Wise, M.J. Rosker and C.L. Tang, J. Chem. Phys., **86**, 2827 (March 1986).
13. "Ultrafast Relaxation Dynamics of Hot Carriers in GaAs and Related Compounds and Structures", C.L. Tang, F.W. Wise and D. Edelstein, Invited Review, Optoelectronics, **1**, 153-162 (Dec. 1986).
14. "Theory of Quantum Beats in Optical Transmission-Correlation and Pump-Probe Measurements", M. Mitsunaga and C.L. Tang, Phys. Rev. A, **35**, 1720 (Feb. 1987).

15. "Transient Optical Pulse Formation and Mode-Locking Through Parametric Traveling-Wave Modulation", T.K. Gustafson, D. Hass, C.L. Tang and J. McLean, Optics Lett., **11**, 219-222 (April 1986).
16. "Polarization Bistability in External-Cavity Semiconductor Lasers", T. Fujita, A. Schremer and C.L. Tang, Appl. Phys. Lett., accepted for publication.
17. "Femtosecond Laser Studies of Ultrafast Processes in Semiconductors and Large Molecules", C.L. Tang, F.W. Wise and I.A. Walmsley, Special Issue on Ultrashort Phenomena and Laser Pulses, Invited, Revue de Physique Applique (Sept. 1987).
18. "Picosecond Relaxation of Hot Carrier Distribution in GaAs/GaAsP Strained-Layer Superlattices", D.C. Edelstein, A.J. Nozik and C.L. Tang, Appl. Phys. Lett., accepted for publication.
19. "Application of Linear Prediction Least-Squares Fitting to Time-Resolved Optical Spectroscopy", F.W. Wise, R.J. Rosker, G.L. Millhauser and C.L. Tang, J. Quant. Elec. (July 1987).
20. "Experimental Determination of Hot-Carrier Scattering Processes in  $\text{Al}_x\text{Ga}_{1-x}\text{As}$ ", F.W. Wise, I.A. Walmsley and C.L. Tang, Appl. Phys. Lett., accepted for publication.
21. "Femtosecond Relaxation Dynamics of Nonequilibrium Carriers in GaAs and Related Compounds and Structures", C.L. Tang, F.W. Wise and I.A. Walmsley, Proc. Fifth Int. Conf. on Hot Carriers in Semiconductors, Boston, MA (July 20-24, 1987).
22. "Ensemble Monte-Carlo Simulations of Femtosecond Energy Relaxation in Bulk GaAs and AlGaAs/GaAs Quantum Well Structures", D. Bailey, C. Stanton, M. Artaki, K. Hess, F. Wise and C.L. Tang, Proc. Fifth Int. Conf. on Hot Carriers in Semiconductors, Boston, MA (July 20-24, 1987).

## **TASK 7    *CARRIER DYNAMICS IN COMPOUND SEMICONDUCTORS STUDIED WITH PICOSECOND OPTICAL EXCITATION***

G.J. Wolga

### **OBJECTIVE**

The objective of this research is to experimentally observe ballistic motion of hot carriers in GaAs using light scattering techniques.

### **APPROACH**

Hot electrons will be injected into GaAs from an GaAs-AlGaAs heterostructure interface in a specially designed device. Sub-bandgap laser radiation will be directed into the device along the direction of motion of the electrons. The back-scattered laser radiation will be spectroscopically examined for a Doppler shifted component indicating a coherent velocity component in the electron flow. The magnitude of the Doppler shift will be a direct measure of the coherent velocity component while the spread in the scattered light spectrum can be correlated with elastic and inelastic collisions that degrade the coherent velocity component.

### **DISCUSSION OF STATE-OF-THE-ART**

Mooradian first observed light scattering from single particle excitations in GaAs using large bulk samples. The transition from single particle to the collective regime was also reported for increasing electron concentrations. Later, Mooradian reported the observation of non-equilibrium velocity distributions in GaAs. Single particle inter-subband scattering in GaAs:AlGaAs heterojunctions has been reported by Abramsohn in 1979. He did not determine electron distribution functions. Prior to our work only Mooradian reported scattering from electrically excited carriers but not for hot electrons.

### **PROGRESS**

In 1984 while working under JSEP support we proposed to study hot electron transport in GaAs by quasi-elastic light scattering from hot electrons in GaAs that were injected into a drift region from a biased AlGaAs:GaAs heterojunction. At that time we predicted that hot electrons drifting through a 0.5 micron thick, lightly doped GaAs slab, could be detected by scattering monochromatic, sub-bandgap light which would reflect a coherent component of electron velocity by a proportional shift in the scattered light frequency. We believed the effect to be observable and that it would provide new and independent evidence of ballistic electron transport over sub-micron dimensions. Our work was not funded by JSEP beyond the first year but, nevertheless, has continued. It is our purpose here to report that substantial evidence has been obtained that we are observing a peak in the electron velocity distribution of the hot, drifting electrons that correlated well with the injection energy. These experiments directly indicate that suitably launched hot electrons in GaAs exhibit drift velocities in the  $(5-10)10^7$ cm/sec range over 0.15 micron distances.

Figure 1 schematically indicates the apparatus we are using. The monochromator, not shown, is a Jobin-Yvon double monochromator, with excellent stray light rejection. It is fitted with a C31034 high quantum efficiency, low noise photomultiplier followed by photon counting electronics. The entire apparatus is

controlled by a computer. Figure 2 is a schematic drawing of the heterojunction electron launching structure which has yielded the best results so far. The upper portion of the figure shows the overall device including the observation window, while the lower portion gives detail on the structure of an individual launcher stack. The electron launcher was grown by MBE in Prof. Lester Eastman's laboratory and processed at Cornell. Scattered light is collected at right angles to the laser beam which propagates perpendicular to the drifting electrons and the scattered light. This geometry helps reduce unwanted stray laser light. Figure 3 shows three superimposed traces of the scattered light spectrum. Trace 1 shows the spectrum with no forward bias applied. It is substantially symmetric on the Stokes and Anti-Stokes sides. Traces 2 and 3 were taken with forward bias applied and each show a peak on the Anti-Stokes side which has shifted farther for larger applied bias (Trace 3 corresponds to greater bias than does Trace 2). These peaks correspond to a coherent component of electron drift velocity imparted by the bias. Scattered light is collected throughout the 1500 Å drift region thus indicating that the electrons remain hot throughout the drift region. The scale on the upper border of Figure 3 gives an indication of the coherent drift velocity we are measuring which approaches  $10^8$  cm/sec. The shape of the electron velocity distribution observed corresponds very well with Monte-Carlo simulations performed in Professor Krusius' group at Cornell (Task 10) on launch structures similar to ours.

New devices have been grown with AlGaAs layers on both sides of a single GaAs drift region to better contain the pump light and with two values of drift region width, 1000 Å and 3000 Å. These have been fabricated for further study. This work demonstrates that quasi-electric light scattering can be an effective, non-invasive probe of hot electron transport in compound semiconductors. We are seeking more detailed knowledge of the dynamics of hot electron transport. Extension of these studies with other launch structures and to transport in real devices and in other materials are other objectives.

#### SCIENTIFIC IMPACT OF RESEARCH

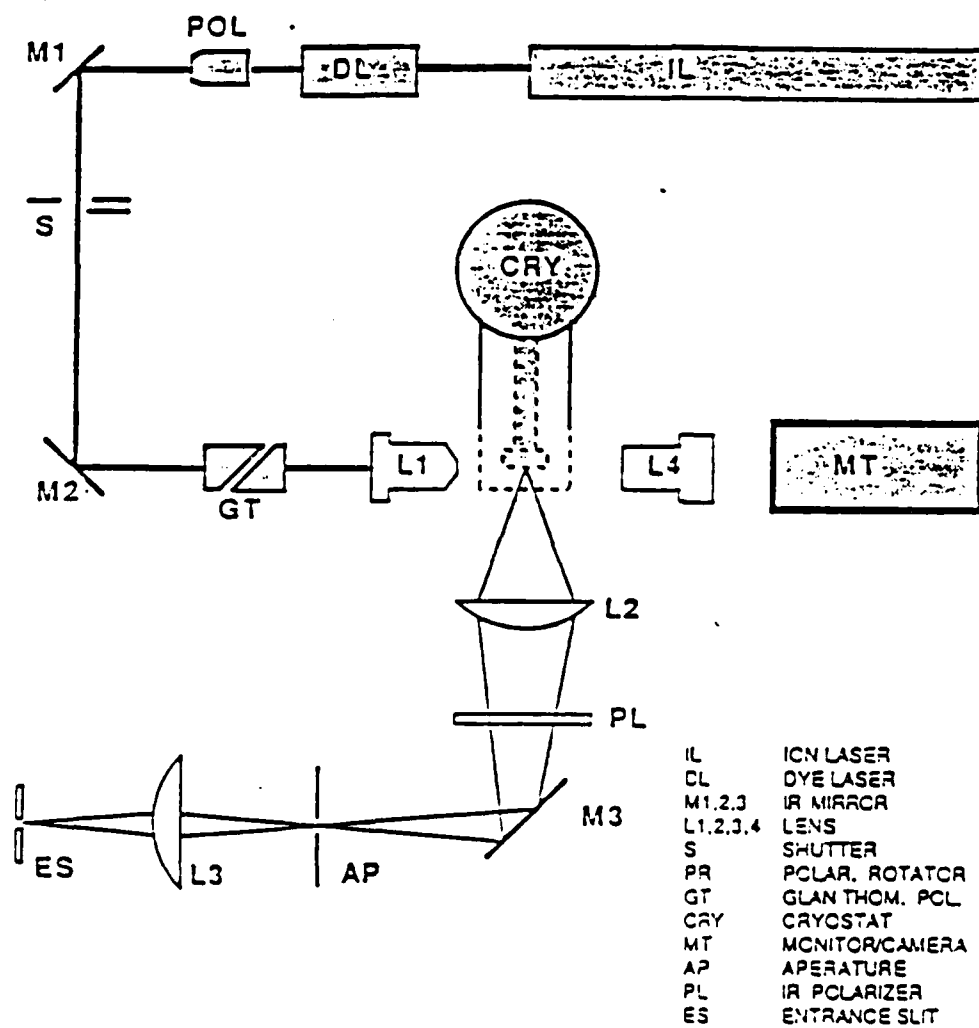
Using single particle scattering in device size structures to determine the distribution function of the carriers will allow the optimization of devices for high speed operation.

#### DEGREES

S.E. Ralph, Ph.D., Sept. 1987


#### JSEP PUBLICATIONS

NONE



90° RAMAN SCATTERING EXPERIMENTAL SETUP

Figure 1



GaAs $n \ 4 \times 10^{17} \text{ cm}^{-3}$	3.0 $\mu\text{m}$
Ballistic launcher stack	3.0 $\mu\text{m}$
GaAs $n \ 4 \times 10^{17} \text{ cm}^{-3}$	4.0 $\mu\text{m}$

25  $\mu\text{m}$

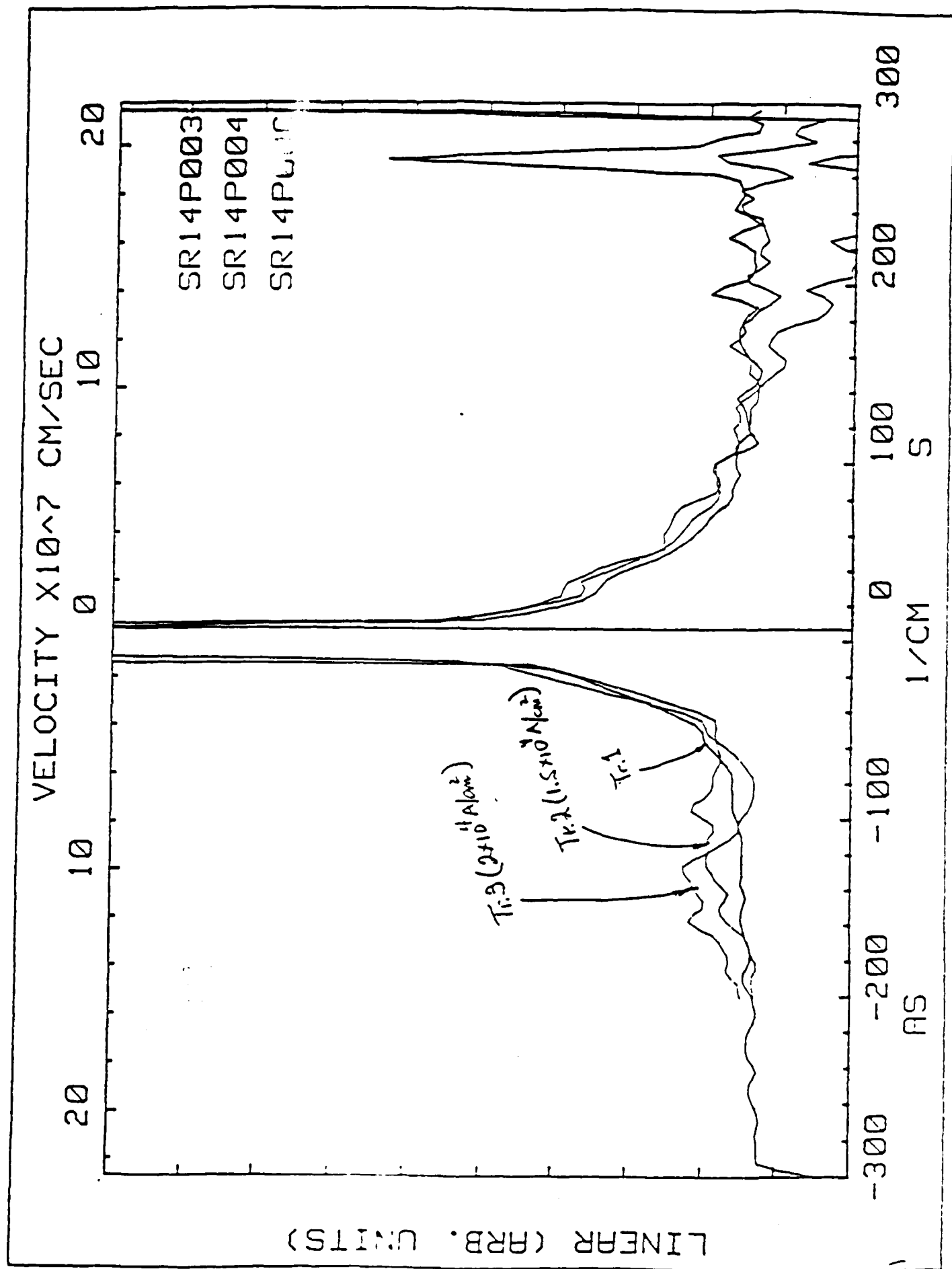
N<sup>+</sup> Substrate



GaAs $n \ 4 \times 10^{17} \text{ cm}^{-3}$	200 Å
graded to AlGaAs $n \ 4 \times 10^{17} \text{ cm}^{-3}$	700 Å
AlGaAs $n \ 1.6 \times 10^{17} \text{ cm}^{-3}$	500 Å
AlGaAs spacer undoped	100 Å
GaAs Drift Region $n \ 1.0 \times 10^{16} \text{ cm}^{-3}$	1500 Å

## HETEROJUNCTION LAUNCHER STRUCTURE

Figure 2





## **TASK 8    *ADVANCED DESIGN TECHNIQUES FOR MICROWAVE GaAs FET AMPLIFIERS***

W.H. Ku

### **OBJECTIVE**

The primary objectives of this research program are to study fundamental device performance and device-circuit interaction for GaAs metal-semiconductor FETs (MES-FETs) and for the higher electron mobility transistor (HEMT), and to develop advanced and integrated analytical and computer-aided design (CAD) techniques for the synthesis and design of GaAs MESFET/HEMT amplifiers, mixers and VCOs leading to monolithic microwave integrated circuits (MMICs) and subsystems. A secondary objective of this research program is to fabricate prototype GaAs MESFET/HEMT amplifiers and circuits in microstrip and monolithic realizations using state-of-the-art submicron gate-length MESFET/HEMTs to verify the integrated design approach developed in the main portion of this 6.1 JSEP program.

It is anticipated that, because of the fundamental nature of this proposed research, the results obtained should have a direct and significant impact on various DOD programs involving ultra-wideband GaAs MESFET/HEMT amplifiers especially in distributed form and MMICs which are directed to ECM and EW system applications and monolithic transceiver modules for phased array applications.

### **DISCUSSION OF STATE-OF-THE-ART**

Tremendous progress has been made over the past several years in low-noise and power GaAs MESFET/HEMT devices and integrated circuits. Low-noise AlGaAs/GaAs HEMTs with submicron gate lengths using optical and e-beam lithography have been reported which can operate at frequencies up to 100 GHz. Power GaAs MESFETs and MISFETs are capable of output powers of hundreds of milliwatts at Ku- and Ka-bands. More significantly, recent advances in monolithic integration of GaAs integrated circuits (ICs) have stimulated great interest in the applications of GaAs ICs for both analog and digital systems.

It is expected that with the advent of monolithic realizations, the complexity of the device and circuit design for GaAs ICs will increase significantly. Techniques common to the design of silicon ICs must be developed for GaAs ICs. We have developed an integrated approach involving both analytical and computer-aided design and synthesis techniques for the design of monolithic GaAs ICs. New and innovative circuit designs including feedback and distributed amplifiers with gain-bandwidth control have been studied. Device physical models for GaAs MESFET/HEMT for both small and large signal, DC and microwave applications have been developed. Nonlinear circuit analysis programs are being developed for the analysis and design of monolithic GaAs MESFET/HEMT device and circuits. An integral part of our technical approach is to verify our designs by the design and actual fabrication of prototype monolithic GaAs MESFET/HEMT circuits.

### **PROGRESS**

Systematic CAD method and general design theory for the GaAs MESFET and HEMT distributed amplifier has been developed. A CAD program to facilitate the design procedure was completed and tested. In keeping with the advances in HEMT

research, a complete I-V model has been developed and subsequently extended in the period to cover the entire range of operation(1), which includes the transconductance compression and subthreshold region. Dual-gate HEMT model has been studied by cascading two single-gate models with a nonlinear algorithm to find the voltage right between the two gates. Excellent agreements are obtained between the measured and modeled I-V characteristics. The nonlinear HEMT model developed in the previous period has been modified to include the breakdown mechanisms and incorporated into the nonlinear program, CADNON. We also employed CADNON to design and simulate a HEMT mixer, which is under fabrication. Progress on the low-noise amplifiers using state-of-the-art quarter-micron HEMT's has been made. Excellent results were obtained for the design of low-noise HEMT amplifiers for millimeter-wave application. Progress of our research is summarized in the following subsections.

(a) Design of Ultra-Wideband Distributed Amplifier Using GaAs MESFETs and HEMTs

The primary objective of this continuing research program is to develop the advanced and integrated analytical theory and computer aided design technique for distributed amplifiers using GaAs MESFETs and HEMTs. The ultimate circuit performance for both small-signal and large-signal applications as well as comparison with other types of amplifiers are to be studied. The distributed GaAs MESFET and HEMT amplifiers are directed toward system applications requiring multi-octave bandwidths.

We have developed the general design theory with gain-bandwidth control for monolithic GaAs MESFET and HEMT distributed amplifiers. The gate line and drain line of the distributed amplifier are designed as a constant-K filter or a Chebyshev filter. At the same time the terminations of gate line and drain line have been redesigned as m-derived sections. In addition, the program of computer aided design for distributed amplifier (DFETA) has been revised with improved convergence speed and extended design options so that the program becomes very user-friendly.

The revised DFETA can predict the gain performance of distributed amplifier exactly and at the same time give optimal gate and drain line structures.

With state-of-the-art quarter micron HEMTs, a 6-stage distributed amplifier covering DC - 60 GHz with 8.5 dB gain and  $\pm 0.5$  dB gain variation has been designed. Quarter micron MESFETs distributed amplifiers covering 2-30 GHz with 9.5 dB gain and  $\pm 0.4$  dB gain variation have been designed. It is believed that this is the widest predicted bandwidth for amplifiers using either GaAs MESFETs or GaAlAs/GaAs HEMTs and any kind of amplifier structures.

(b) Nonlinear HEMT Modeling

An analytical and CAD model for HEMT I-V characteristics has been developed and under constant modification. This model was derived based upon the approximate solution of the electron transport equations in a GaAlAs/GaAs heterojunction and it includes velocity saturation effects, drain feedback effects, channel modulation effects, and a parasitic MESFET in the AlGaAs layer. Using this compact and flexible I-V model, we were able to simulate I-V characteristics of some state-of-the-art quarter-micrometer gate HEMTs with excellent results, including devices from GE, TRW, Rockwell and Cornell. We also studied the dual-gate model

by cascading two single-gate model. The floating voltage between the two gates was determined by a nonlinear algorithm. To verify the accuracy of the nonlinear HEMT model based on the I-V model, bias-dependent S-parameters were used to characterize the model and the S-parameters at different bias generated from the nonlinear model was then compared to the original S-parameters. The agreement between the measurement and model was excellent.

The model was incorporated into the nonlinear time domain program, CADNON, and will be used to simulate HEMT nonlinear circuits such as HEMT mixers, HEMT distributed amplifiers, and double heterojunction HEMT power amplifiers. These HEMT nonlinear circuit simulations will investigate the ultimate performance of HEMT under large-signal operation.

Since all these models were developed based on device physical model instead of phenomenological nature, the device performance are closely related to the physical parameters used in the models. Hence, we can predict the behavior of the device before fabrication and the optimal device structures such as doping concentrations and heterojunction and super-lattice layer structures to be grown by MBE can be determined.

#### (c) Design and Simulation of Nonlinear Circuits

A complete simulation on HEMT mixer to study the capability of the HEMT as a mixer. With the systematic design method based on the nonlinear program CADNON, we have designed mixers using state-of-the-art GE devices with higher conversion gains than reported for GaAs MESFET mixers. Typical results are conversion gains 10 dB at 40 GHz, 4 dB at 20 GHz, and -2 dB at 40 GHz, where the intermediate frequency is set at 2 GHz. Since our HEMT I-V model is capable of modeling the transconductance compression, whose effects on the performance of a HEMT mixer has been investigated, including the anomalous bias dependency of the conversion gain (Figure 1) and reduction of the maximum conversion gain. Detailed study concerning the way device parameters influence the mixer performance has been made. The results provide a guideline to optimize the HEMT for mixer application.

Design methods for MESFET power amplifiers and VCOs based on the new version of CADNON were also studied. The optimum load condition for a power amplifier can be determined from the perturbation analysis provided by CADNON. Based upon this information, the matching network for power amplifiers and embedding networks for oscillators can be designed using a linear circuit synthesis program such as CADSYN<sup>TM</sup>. It is expected that the systematic design methods for specified nonlinear circuits will soon be completed.

#### (d) Noise Theory and Design of Low-Noise Broadband Amplifier Using AlGaAs/GaAs HEMTs

Analytical and computer aided design methods for broadband Low-Noise Amplifiers (LNA) have been extended to sub-half-micron gate AlGaAs/GaAs HEMT devices. An accurate noise model<sup>(2)</sup> is indispensable in all the low noise amplifier design. Owing to the complicated physical random process involved in the HEMT structure especially when the gate length is short, we can only obtain a simplified but reliable noise model suitable for low noise amplifier design (Figure 2). The development of a more complete model including the hot electron effect and the spatial correlation of the random noise source is currently underway. To investigate the superior noise property of HEMT at Ka band (26.5 GHz-40 GHz), a two-state low-

noise amplifier (Figure 3) using GE 0.25 micron x 150 micron HEMT with minimum noise figure 1.8 GHz at 30 GHz has been designed with a predicted gain of  $18 \pm 0.4$  dB for 20 to 40 GHz band and a maximum noise figure of 2.8 dB at the high frequency end. In comparison with the monolithic GaAs MESFET LNA for Ka band recently fabricated by Hughes, with an average noise figure of 7 dB and an associated gain of 14 dB(2) this is believed to have the best performance for any solid-state device covering this frequency range. The 20-40 GHz low-noise HEMT amplifier is planned to be fabricated in the near future.

#### DEGREES

Guan-wu Wang, M.S., January 1986

"An Analytical and Computer Aided Model for the High Electron Mobility Transistor"

Dean Barker, M.Eng., August 1985

"Design of Low Noise HEMT Amplifiers"

#### PUBLICATIONS

1. G-W. Wang and W.H. Ku, "Analytical and Computer Aided Model of the AlGaAs/GaAs High Electron Mobility Transistor", IEEE Trans. Elec. Dev., ED-33 (5) 657-663 (May 1986).

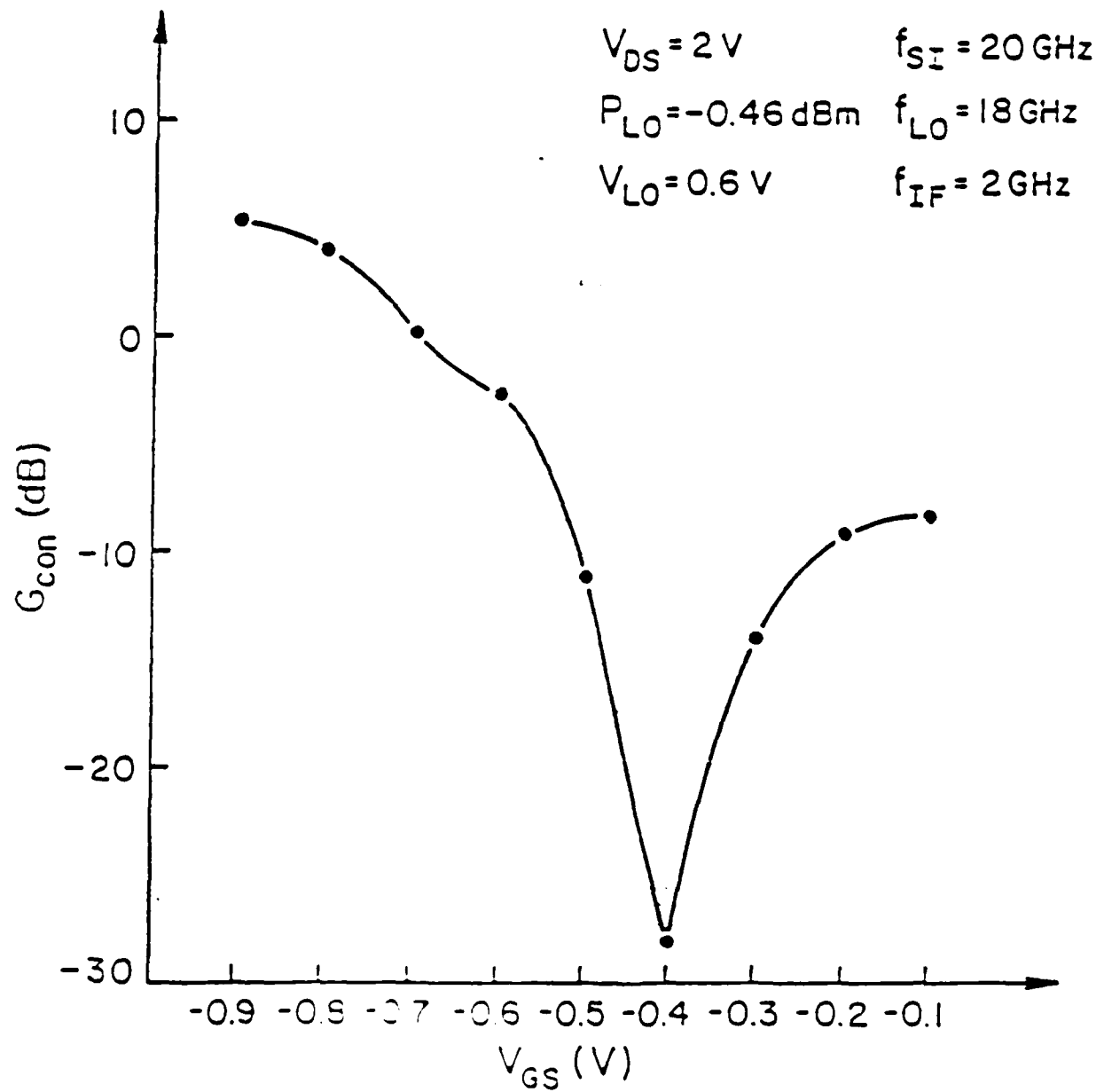


Figure 1: Conversion Gain vs Gate Bias of the 20 GHz HEMT Mixer

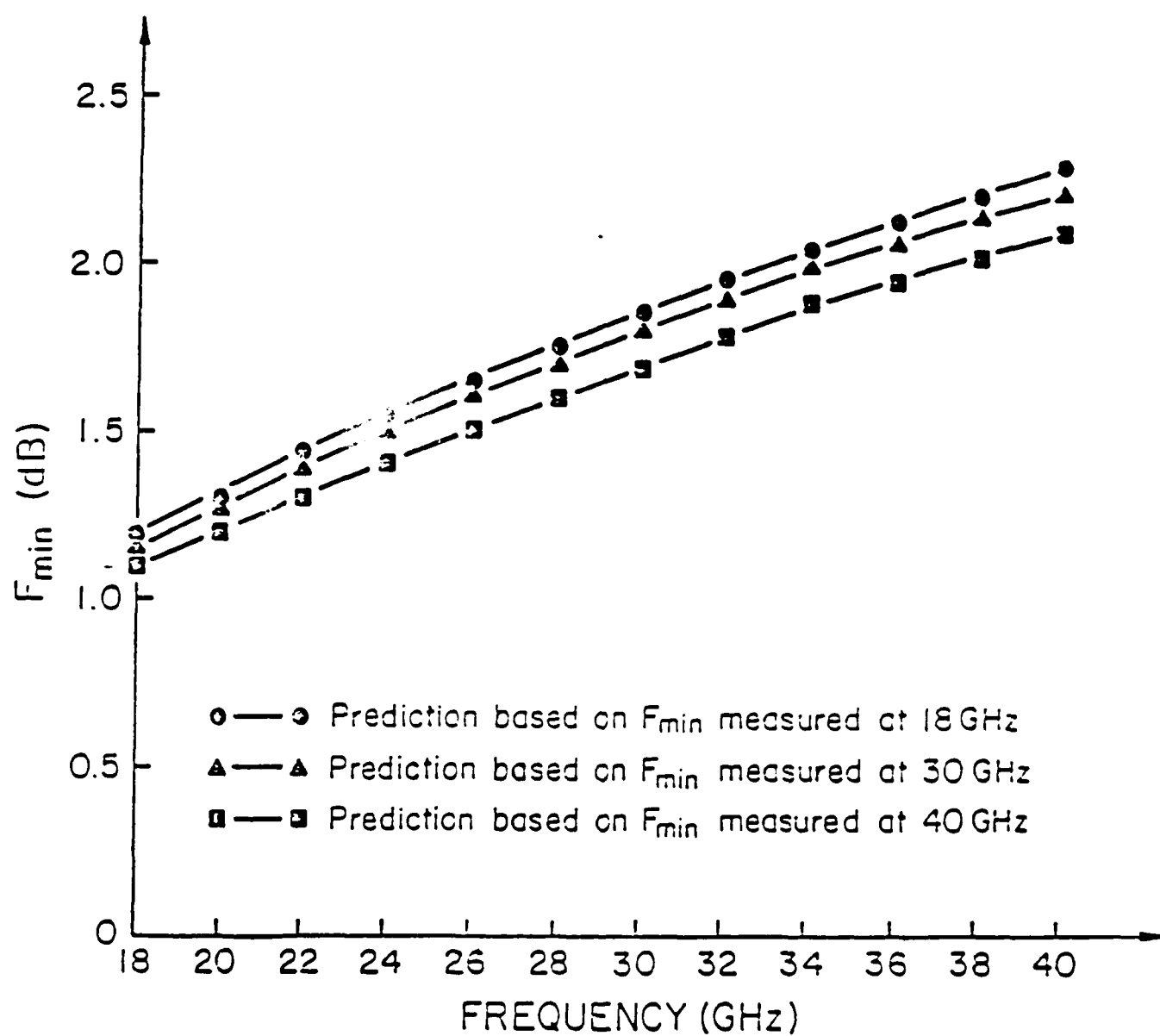


Figure 2: Minimum Noise Figure of the GE HEMT Calculated by Noise Model

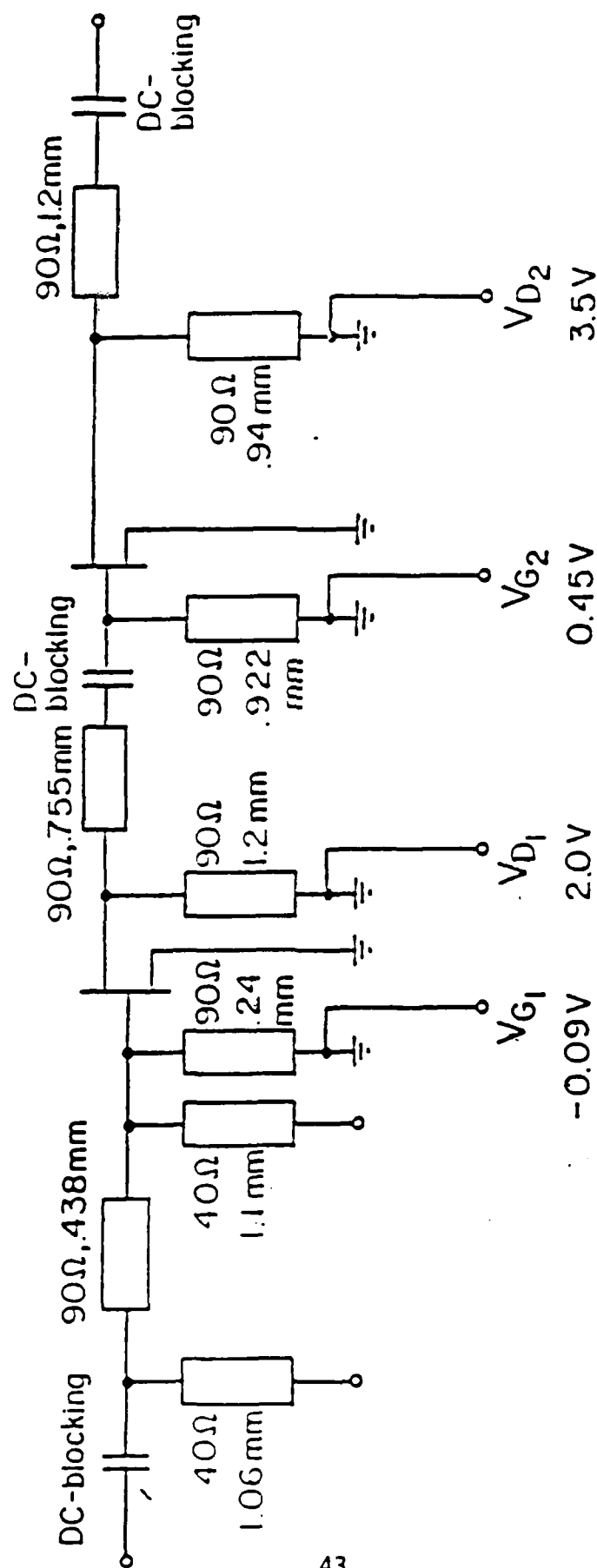


Figure 3: Circuit Diagram of 20 GHz 2 Stage HEMT LNA

## **TASK 9    WIDEBAND CIRCUITS AND SYSTEMS**

H.J. Carlin

### **OBJECTIVE**

Fundamental research on the application of gain bandwidth theory to design of wideband systems.

### **APPROACH**

Basic network theory is used to obtain fundamental limitations, design methods, and practical models for microwave circuits and optical waveguide.

### **PROGRESS**

A new and far-reaching fundamental result governing the optimum behavior of wideband amplifiers has been obtained. A comprehensive paper, "On Flat Gain with Frequency Dependent Terminations", by H.J. Carlin and Pier Civalleri, was published in IEEE Trans. CAS, August 1985.

A new approach to modeling graded index optical guide with particular emphasis on dispersion analysis has been completed. A full paper was presented at the IEEE MTT Symposium in St. Louis June 1985, "A New Approach to Dispersion Analysis in Graded Index Optical Fiber", by H.J. Carlin and Henry Zmuda.

### **DEGREES**

1. Henry Zmuda, Ph.D., July 1984  
"A New Approach to Dispersion Analysis in Graded Index Optical Fibers"
2. Christopher Near, M.S., January 1985  
"Flat Gain Limitations in Complex Generator-Load Systems"

### **JSEP PUBLICATIONS**

1. "On Flat Gain With Frequency Dependant Terminations", H. Carlin and P. Civalleri, IEE Trans.-CAS (Aug. 1985).
2. "A New Approach to Dispersion Analysis in Graded Index Optical Fibers", H. Carlin and H. Zmuda, Proc. IEEE MTT Symp., St. Louis, MO (June 1985).
3. "Double Broadband Matching and the Problem of Reciprocal Reactance 2- $\mu$ m Port Cascade Decomposition", D.C. Youla, H.J. Carlin and B.S. Yarman, Int. J. Circuit Theory and Applications, 12 (3) 269-281 (July 1984).



## **TASK 10 , DEVICE SIMULATION AND CIRCUIT MODELING FOR III-V DEVICES IN THE BOUNDARY LIMITED HIGH FIELD TRANSPORT REGIME**

J.P. Krusius

### **OBJECTIVE**

The objective of this project, over the period from May 1984 to April 1987, was to explore theoretically the characteristics of small high speed III-V compound semiconductor devices in a regime, where carrier transport is determined by transient phenomena and boundaries. Since in this domain the carrier distribution function is a priori unknown, particle methods have been used exclusively. Microscopic and macroscopic transport issues have been explored in small inhomogeneous binary and graded ternary compound semiconductors. The  $\text{Al}_x\text{Ga}_{1-x}\text{As}/\text{GaAs}$  materials system has been selected as the primary demonstration case.

### **DISCUSSION OF STATE-OF-THE-ART**

Control of energy bands and interfaces in compound semiconductor heterostructures and superlattices combined with submicron lithographies has facilitated a host of new high speed device structures. The physics these device structures is characterized by a mixture of microscopic classical scale phenomena and semi-classical atomic scale phenomena with the relative importance of each class varying from case to case. Since the dimensions of most future electronic and optoelectronic devices are in the submicron size scale, the understanding of the complex device physics phenomena is crucial for the evolution of new concepts and applications in the field of compound semiconductor devices. Significant efforts to advance the understanding of high speed device physics phenomena have been timely for a number of years because of the recently achieved control of the characteristics of compound semiconductor heterostructures and the emerging wealth of measured electrical and complementary optical data.

A number of important problems in the physics of submicron compound semiconductor heterostructures were identified in 1984, when this study was started: (1) carrier transport in small structures subject to boundaries, (2) carrier transport in structures with a position dependent composition, and (3) high energy carrier injection from thermionic and tunnel emitters.

- (1) Carrier transport in small structures cannot be decoupled from confining quantum mechanical boundaries and thermodynamically open boundaries, when the mean free path is comparable to, or larger than, the minimum dimensions. In such cases quantum mechanical confining boundaries will alter the available carrier states. For other types of boundaries the carrier distribution function is established on one hand by internal carrier-lattice and carrier-carrier interactions, and the other hand by carrier-boundary or external reservoir interactions. The postulated characteristics for these reservoirs will then serve to establish "boundary conditions" for the distribution function. Carrier transport subject to quantum mechanical confining boundaries at compound semiconductor heterointerfaces in single wells has been studied 1986 by K. Yokoyama and K. Hess [1]. The significance of thermodynamically open boundaries on carrier transport in small structures was recognized by A. Al-Omar and J.P. Krusius (JSEP Publication 4) and W. Frensley [2] in 1986. The former explored carrier exchange phenomena at the interface between a compound semiconductor and a Maxwellian outside reservoir with a slightly

drifted distribution function, and established proper Poisson injection statistics for particle exchange with the reservoir. This allows fluctuations and transient phenomena to be included (JSEP Publication 1). Distribution functions were shown to be significantly influenced by the collecting and injecting boundaries. W. Frensley postulated the existence of open thermodynamic boundaries as a necessity for obtaining meaningful results in his Wigner function solution for the resonant tunneling effect [2].

- (2) Band parameter tailoring in modern compound semiconductor heterostructures leads to position dependent compositions. Carrier transport has to be described in a medium, in which electron states, phonon spectra, and trap characteristics have become functions of position in addition to the existence of atomically sharp heterojunctions. Compositional grading by necessity also leads to compositional disorder of cations or anions in ternary and quaternary compound semiconductors. Since compositional grading changes, for example, effective masses and scattering rates, its inclusion is important for the proper description of carrier dynamics. Transport in ternary structures with sharp step-type heterojunctions has been explored previously using macroscopic drift-and-diffusion methods in 1984 [3] and microscopic Monte Carlo particle methods by a Japanese group in 1985 [4] parallel to our effort. The Japanese group extended a traditional ensemble Monte Carlo formulation to stepped heterostructures without detailed considerations for the underlying physics. Hot electron transport in graded structures involving gradually changing cation compositions in addition to sharp heterojunctions has been studied only by Al-Omar and J.P. Krusius (JSEP Publications 5-8). They have formulated a new transport description based on  $k \cdot p$  interpolated electron states and properly symmetrized overlap integrals for graded ternary heterostructures with imbedded sharp heterostructures. These authors also derived the minimum critical length scale for the validity of the  $k \cdot p$  based electron dynamics using perturbation theory.
- (3) High energy electron injection from heterojunctions has been one of the key concepts for enhancing electron velocities and generating near ballistic electrons. This concept has been applied, e.g. to the heterojunction bipolar transistor already in 1982 [5] and to the tunneling hot electron transfer amplifier in 1985 [6]. The injection process for thermionic step junctions was originally, prior to our effort, explored by Tang and Hess using a single particle Monte Carlo formulation in 1982 [7]. Tomizawa and Awano in 1985 included carrier ensemble effects with step junctions but did not explore the details of the injection process [4]. Al-Omar and Krusius reconsidered the injection process by including cation grading, ensemble phenomena, and all space charge effects using their new transport formulation (JSEP Publications 5,8) in 1986. Space charge effects on the injection turned out to be crucial. Conditions for flat band at the injecting heterojunction as a function of cation grading, transport, temperature, and applied voltage were derived both from the self-consistent ensemble calculations and a simple intuitive equation based on injection and drift current ratio. Average velocities and ballistic electron fractions were shown to vary by a factor of four depending on the state of the heterojunction. Tunneling type hot electron emitters have not been described until 1986 with the  $k \cdot p$  interpolation formulation but neglecting all scattering and space charge phenomena [2,3].

## PROGRESS

The present effort focused primarily on the physics of carrier launching and collection mechanisms under high field conditions in simple, small size, inhomogeneous, high speed compound semiconductor structures with a position dependent composition. The approach taken was to simultaneously include as much of the essential microscopic and macroscopic physics as possible, in order to be able to perform correlations with measured data, and not to refine the treatment of one particular issue as far as possible. Device physics issues beyond carrier dynamics and scattering that have been included here are full time-dependence, large signal transient phenomena, self-consistent fields, carrier ensemble phenomena, graded heterojunctions, and device-boundary interactions. The following results have been obtained.

### (1) Transport Formulation

A new time-dependent hot electron transport formulation for the self-consistent semi-classical ensemble Monte Carlo method suitable for graded compound semiconductor devices has been developed. This formulation includes a number of significant new physical phenomena. Energy bands, phonon spectra, and scattering processes are treated position dependent. The d.p interpolation method is used to model the position dependent energy bands. Scattering rates are calculated using overlap integrals with proper symmetry characteristics. Ionized impurity scattering, based on Ridley's reformulation of the Brooks-Herring scattering matrix with collective effects and overlap integrals, has been employed. Compositional cation disorder enters via alloy scattering. Degenerate statistics and freeze out for impurities, quantum mechanical reflection at interfaces, and contact resistances have also been included. Perturbation theory has been used to derive a new expression for the critical minimum length scale, which establishes the validity range of this formulation. Device boundaries are open in the thermodynamic sense and allow the device to interact with outside reservoirs postulated to be in thermodynamic equilibrium. Consequently we can describe full carrier exchange processes at device contacts including, for example, transient states of the device violating charge neutrality and noise phenomena. The details of this transport formulation have been documented in JSEP publications 4 and 5.

### (2) Algorithms and Software

New momentum and energy conserving algorithms have been developed in order to integrate the equations of motion of electrons with position dependent dynamics and over abrupt heterojunctions. The above transport formulation has been implemented in our time-dependent large signal self-consistent Monte Carlo computer code for one-dimensional ternary compound semiconductor devices (TCMC). The first and second generation versions of this code are running on the HARRIS 800 and DEC MicrovaxII minicomputers respectively. The code has been calibrated against measured drift velocity-electric field distributions with and without overlap integrals. A port to the Cornell production supercomputer (IBM 3090-600, FPS 264/164's) is in progress (version 3.0). A two-dimensional implementation of our self-consistent Monte-Carlo formulation is in progress as well.

### (3) Device Applications

Device-reservoir interactions have been studied in short one-dimensional GaAs resistors and ballistic  $\text{Al}_x\text{Ga}_{1-x}\text{As}/\text{GaAs}$  diodes in order to study the coupling between transport and device interfaces for open systems. The calculated distribution functions show strong non-Maxwellian boundary effects. Results have been published (JSEP publication 4).

Injection of ballistic electrons from the  $\text{Al}_x\text{Ga}_{1-x}\text{As}/\text{GaAs}$  heterointerface into GaAs drift regions has been explored in order to establish the decay length and the ballistic electron fraction. The distribution function as a function of position has been calculated. Ballistic electron decay lengths of 250 and 150 nm have been found for 77 and 300 K respectively. The width of the ballistic electron distributions is on the order of two optical phonon energies and carries up to 80 per cent of the electrons passing the ballistic injector. These results are documented in JSEP publications (3-5).

Real time oscillations in Gunn diodes with heterojunction cathodes have been explored with our new formulation using time dependent large signal boundary conditions in collaboration with an experimental device fabrication effort in Prof. L. Eastman's group. Our tentative simulations explain the measured power conversion enhancement by a factor of 3 for  $\text{AlGaAs}/\text{GaAs}$  heterojunction cathode Gunn diodes. Results indicate that earlier predictions for the frequency limitations of Gunn diodes are too conservative. Heterojunction cathode Gunn diodes show a considerable shortening of the dead zone via electron transfer across the heterojunction and thus exhibit gain at higher frequencies than earlier believed. Detailed results will be presented at the 1987 Cornell Conference (JSEP publication 7).

A detailed study of one-dimensional thermionic ternary/binary heterojunction electron injectors of the generic  $\text{A}_x\text{B}_{1-x}\text{C}/\text{DE}$  type is under way. Space charge, cation grading, temperature and applied voltage effects on the injection process and the resulting self-consistent electron distribution function are being explored. Preliminary results will be presented at the 5th International Conference on Hot Carriers in Semiconductors, July 1987 (JSEP publication 6) and more extensive publication will be submitted as well (JSEP publication 8). These results show the crucial need to incorporate space charges into the theory of small compound semiconductor structures. The existence of flat band conditions at such a heterojunction depends on a complicated injection/drift current ratio, and average velocities downstream from the heterojunction may vary by a factor of four depending on the charge state of the heterojunction.

### SCIENTIFIC IMPACT OF RESEARCH

Our new transport formulation allows to analyze time-dependent hot carrier transport in graded ternary heterostructures with imbedded heterojunctions. All significant semiclassical microscopic processes have been included. The present transport formulation and its Monte Carlo implementation thus provides an ideal tool for realistically analyzing complex interactions of device physics phenomena in a large number of small inhomogeneous high speed devices and then correlate results with measured data. Applications studied to date show that new insight and new device designs have already emerged and more will follow. We also plan to release our time-dependent self-consistent ternary compound semiconductor ensemble Monte Carlo code for the benefit of other researchers in the field.

## DEGREES

Two graduate students, A. Al-Omar and S. Weinzierl, have been involved in this research in addition to the principal investigator. A. Al-Omar is expected to complete his Ph.D. thesis

A. Al-Omar, Transient Transport in Small Graded Compound Semiconductor Devices, Ph.D. Thesis in preparation under direction of J.P. Krusius

in January 1988. S. Weinzierl started his combined Master of Science/Doctor of Philosophy program in September 1986 and still has several years until completion.

## REFERENCES

1. "Monte Carlo Study of Electronic Transport in  $\text{Al}_x\text{Ga}_{1-x}\text{As}/\text{GaAs}$  Single Well Heterostructures", K. Yokoama and K. Hess, Phys. Rev., **833** (8) 5595 (1986). "Calculation of Warm Electron Transport in  $\text{AlGaAs}/\text{GaAs}$  Single Heterostructure Using a Monte Carlo Method", I. Yokoama and K. Hess, J. Appl. Phys., **59** (11) 3798 (1986).
2. "Transient Response of a Tunneling Device Obtained from the Wigner Function", R. Frensley, Phys. Rev. Lett., **57** (22) 2853-2856 (1986).
3. "Thermionic Emission-Diffusion Theory of Isotype Heterojunctions", R.J. Shuelke and M.S. Lundstrom, Solid State Elec., **27** (12) 1111-1116 (1984).
4. "Simulation of Near Ballistic Electron Transport in Submicron  $\text{GaAs}$  Diode with  $\text{Al}_{(x)}\text{Ga}_{(1-x)}\text{As}/\text{GaAs}$  Heterojunction Cathode", K. Tomizawa, Y. Awano, N. Nashizume and M. Kawashima, IEE Proc., Part I, **132**, p. 37 (1985).
5. " $\text{GaAlAs-GaAs}$  Ballistic Heterojunction Bipolar Transistor", D. Ankri and L.F. Eastman, Elec. Lett., **18**, 750 (1982).
6. "Direct Observation of Ballistic Transport in  $\text{GaAs}$ ", M. Heiblum, M. Nathan, D.C. Thomas and C.M. Knoedler, Phys. Rev. Lett., **55**, 2200 (1985).
7. "Investigation of Transient Electronic Transport in  $\text{GaAs}$  Following High Energy Injection", J. Tang and K. Hess, IEEE Trans. Elec. Dev., **ED-29**, 1906 (1982).
8. "Wigner Function Simulation of Quantum Tunneling", N. Kluksdahl and D.K. Ferry, Third Int. Conf. of Superlattices, Microstructures and Microdevices, Chicago, IL (Aug. 1987).

## JSEP PUBLICATIONS

1. "Boundary Effects on Stationary and Transient Characteristics of  $\text{GaAs}$  Device Structures", A. Al-Omar and J.P. Krusius, 1985 IEEE/Cornell Conf. on Advanced Concepts for High Speed Semiconductor Devices and Circuits, IEEE, NY, 240-245 (1985).

2. "Ensemble Monte Carlo Study of Heterojunction Launchers", A. Al-Omar and J.P. Krusius, 8th Industrial Affiliates Meet. of Program for Submicrometer Structures, 2 page summary (Oct. 1986).
3. "Study of Heterojunction Launchers for Generation of Ballistic Electrons", A. Al-Omar and J.P. Krusius, Proc. Int. Elec. Dev. Meet., IEEE, 85-88 (1986).
4. "Boundary Limited Transport in Ultra Small Devices", A. Al-Omar and J.P. Krusius, Proc. First Int. Conf. on Numerical Modeling of Semiconductor Devices, Boole Press, Dublin, Ireland, Ed. J.J.M. Miller, pp. 3-9 (1987).
5. "Self-Consistent Monte Carlo Study of High Field Carrier Transport in Graded Heterostructures", A. Al-Omar and J.P. Krusius, J. Appl. Phys., to appear in Oct. (1987 issue).
6. "Microscopic Transport in Graded Heterostructures", A. Al-Omar and J.P. Krusius, Fifth Int. Conf. on Hot Carriers in Semiconductors (July 1987), accepted for publication, to appear in proceedings (special issue in Solid State Electronics).
7. "Space Charge Effects in Heterojunction Cathode (Al:Ga)As Gunn Oscillators", A. Al-Omar, J.P. Krusius, Z. Greenwald, A.R. Calawa and L.F. Eastman, Eleventh Biennial IEEE/Cornell Conf. on Advanced Concepts in High Speed Semiconductor Devices and Circuits (Aug. 1987) in press.
8. "Conditions for Space Charge Reversal at Thermionic Heterojunctions Designed for Ballistic Electron Injection", A. Al-Omar and J.P. Krusius, submitted to IEEE Elec. Dev. Lett. (July 1987).

ALL INFORMATION CONTAINED HEREIN IS UNCLASSIFIED  
DATE 10-10-80 BY 1040  
EXCEPT WHERE SHOWN OTHERWISE AND IS  
THE PROPERTY OF THE AIR FORCE RESEARCH  
LABORATORIES HURLER HAFB AFM 19-12.  
THIS DOCUMENT IS UNCLASSIFIED  
DATE 08-01-80 BY 1040  
EXCEPT WHERE SHOWN OTHERWISE  
AND IS THE PROPERTY OF THE  
AIR FORCE RESEARCH  
LABORATORIES HURLER HAFB AFM 19-12.  
UNCLASSIFIED INFORMATION DIVISION

ALL INFORMATION CONTAINED  
HEREIN IS UNCLASSIFIED  
DATE 08-01-80 BY 1040  
EXCEPT WHERE SHOWN OTHERWISE  
AND IS THE PROPERTY OF THE  
AIR FORCE RESEARCH  
LABORATORIES HURLER HAFB AFM 19-12.  
UNCLASSIFIED INFORMATION DIVISION

END

DATE

FILMED

5-88  
DTIC